7202 J. Med. Chem. 2010, 53, 7202–7218
DOI: 10.1021/jm100863x

Journal of Medicinal Chemistry Article

Discovery of a β-D-2′-Deoxy-2′-α-fluoro-2′-β-C-methyluridine Nucleotide Prodrug (PSI-7977) for the Treatment of Hepatitis C Virus

Michael J. Sofia,* Donghui Bao, Wonsuk Chang, Jinfa Du, Dhanapalan Nagarathnam, Suguna Rachakonda, P. Ganapati Reddy, Bruce S. Ross, Peiyuan Wang, Hai-Ren Zhang, Shalini Bansal, Christine Espiritu, Meg Keilman, Angela M. Lam, Holly M. Micolochick Steuer, Congrong Niu, Michael J. Otto, and Phillip A. Furman

Pharmasset, Inc., 303A College Road East, Princeton, New Jersey 08540

Received July 10, 2010

Hepatitis C virus (HCV) is a global health problem requiring novel approaches for effective treatment of this disease. The HCV NS5B polymerase has been demonstrated to be a viable target for the development of HCV therapies. β-D-2′-Deoxy-2′-α-fluoro-2′-β-C-methyl nucleosides are selective inhibitors of the HCV NS5B polymerase and have demonstrated potent activity in the clinic. Phosphoramidate prodrugs of the 5′-phosphate derivative of the β-D-2′-deoxy-2′-α-fluoro-2′-β-C-methyluridine nucleoside were prepared and showed significant potency in the HCV subgenomic replicon assay (<1 μM) and produced high levels of triphosphate **6** in primary hepatocytes and in the livers of rats, dogs, and monkeys when administered in vivo. The single diastereomer **51** of diastereomeric mixture **14** was crystallized, and an X-ray structure was determined establishing the phosphoramidate stereochemistry as *S*p, thus correlating for the first time the stereochemistry of a phosphoramidate prodrug with biological activity. **51** (PSI-7977) was selected as a clinical development candidate.

Introduction

The hepatitis C virus (HCV[a]) presents a global health problem with approximately 180 million individuals infected worldwide with 80% of those progressing to chronic HCV infection.[1] Of those chronically infected individuals, approximately 30% will develop liver cirrhosis and 10% will go on to develop hepatocellular carcinoma.[2] The current standard of care (SOC) for HCV infected patients consists of regular injections of pegylated interferon (IFN) and oral ribavirin (RBV) administration. However, SOC has proven to be effective in producing a sustained virological response in only 40−60% of patients treated, dependent on viral genotype and other predictors of host immune responsiveness. In addition, drug discontinuations may be high because of adverse side effects associated with the SOC treatment regimen.[3,4] Consequently, the development of alternative treatment options is greatly needed. The search for novel therapies for the treatment of HCV infection has focused on the development of direct acting antiviral agents (DAAs).[5,6]

HCV is a plus strand RNA virus of the *Flaviviridea* family with a 9.6 kb genome encoding for 10 proteins: three structural proteins and seven nonstructural proteins. The nonstructural proteins, which include the NS5B RNA dependent RNA polymerase (RdRp), provide several attractive targets for the development of anti-HCV therapy.[7,8] The HCV RdRp is part of a membrane associated replication complex that is composed of other viral proteins, viral RNA, and altered cellular membranes.[3] The NS5B polymerase is responsible for replicating the viral RNA genome and thus is absolutely required for HCV replication. As in the case of other viral polymerases, two approaches have been pursued to identify small molecule HCV NS5B polymerase inhibitors. These approaches include the identification of nucleoside analogues that function as alternative substrate inhibitors that induce a chain termination event and non-nucleoside inhibitors that bind to allosteric sites on the polymerase leading to a nonfunctional enzyme.[5,6]

Several nucleoside classes have been or continue to be in development as inhibitors of HCV. These classes include the β-D-2′-deoxy-2′-α-F-2′-β-C-methylribose, the β-D-2′-β-methylribose, and the 4′-azidoribose classes.[9−13] These classes are represented by the clinical candidates **1** (RG7128), **2** (NM-283), and **3** (R1626), respectively (Figure 1).

Compound **1** is a 3′,5′-diisobutyrate ester prodrug of the cytidine nucleoside **4**. In clinical studies when administered at 1000 mg b.i.d., **1** demonstrated efficacy in genotype 1 infected patients (reduction of HCV RNA levels) in a 14-day monotherapy study (−2.7 $\log_{10}$ decrease in HCV RNA) and produced a 88% RVR in a 4-week combination study with SOC−pegylated interferon plus ribavirin.[14,15] In addition, **1** was shown to be efficacious in HCV genotype 2,3 patients who had not responded to prior therapy, the first direct-acting

*To whom correspondence should be addressed. Phone: (609) 613-4123. Fax: 609-613-4150. E-mail: michael.sofia@pharmasset.com.

[a] Abbreviations: HCV, hepatitis C virus; SOC, standard of care; IFN, interferon; RBV, ribavirin; DAA, direct acting antiviral; RdRp, RNA dependent RNA polymerase; b.i.d., twice daily; q.d., once daily; YMPK, uridine−cytidine monophosphate kinase; NDPK, nucleoside diphosphate kinase; SAR, structure−activity relationship; NMI, *N*-methylimidazole; DCM, dichloromethane; EC_{90}, compound concentration that returns 90% of inhibition; SGF, simulated gastric fluid; SIF, simulated intestinal fluid; NTP, nucleoside triphosphate; PK, pharmacokinetic; C_{max}, maximum concentration; AUC, area under the curve; t_{max}, time at maximum concentration; PAMPA, parallel artificial membrane permeability assay; IC_{50}, compound concentration that returns 50% of inhibition; NOAEL, no observed adverse effect level; TFA, trifluoroacetic acid, THF, tetrahydrofuran; IPE, isopropyl ether; DMSO, dimethylsulfoxide.

 Published on Web 09/16/2010

antiviral to show multiple genotype coverage in the clinic.[16] However, even with the positive clinical attributes of **1**, we were interested in investigating second generation agents with improved potency, enhanced pharmacokinetic properties (i.e., q.d. dosing), and the potential for generating high concentrations of the active triphosphate in the liver to enable low doses and potentially fixed-dose combinations of DAAs. To achieve this objective, we focused on β-D-2′-deoxy-2′-α-F-2′-β-*C*-methyluridine (**5**) (Figure 2). Earlier studies had shown that while **5** was inactive in the HCV replicon assay, its triphosphate was a potent inhibitor of HCV NS5B with a K_i of 0.42 μM.[17−19] In addition, metabolism studies with **4** showed that the monophosphate of **4** can be deaminated to the uridine monophosphate derivative and subsequently anabolized to the triphosphate **6** by uridine−cytidine monophosphate kinase (YMPK) and nucleoside diphosphate kinase (NDPK) (Figure 2). This uridine triphosphate was shown to have an intracellular half-life of 38 h.[17−19] Therefore, in order to leverage the desired attributes of the uridine derivative, we needed to deliver the monophosphate of uridine nucleoside **5**. To accomplish this, we required a monophosphate prodrug that would bypass the nonproductive phosphorylation step and that would potentially accomplish our other objective: the delivery of high liver concentrations of the desired triphosphate **6**.

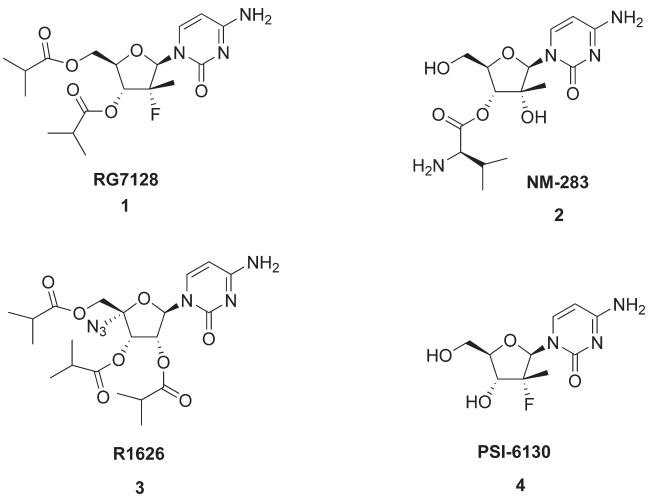

Figure 1. Structures of HCV nucleoside inhibitors **1**, **2**, **3**, and **4**.

Phosphoramidate prodrug strategies had been shown to enhance nucleoside potency in cell culture presumably by increasing intracellular concentrations of the active nucleotide.[20−22] However, at the time we began our work there was no example where phosphoramidate prodrug technology was applied to the inhibition of HCV. We speculated that application of the phosphoramidate prodrug method would be an ideal approach for delivering the desired uridine monophosphate to hepatocytes in an in vivo setting (Figure 3). We hoped to take advantage of first pass metabolism where the liver enzymes would hydrolyze the terminal carboxylic acid

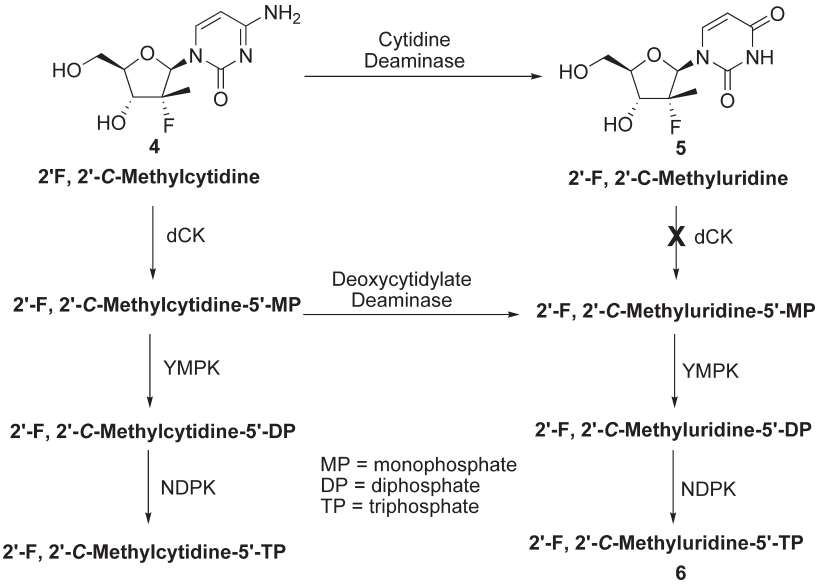

Figure 2. Metabolism of **4** leads to both the active triphosphate and the inactive nucleoside **5**. The monophosphate metabolite of **4** is also metabolized to the uridine monophosphate derivative which is then further phosphorylated to the active uridine triphosphate **6**.

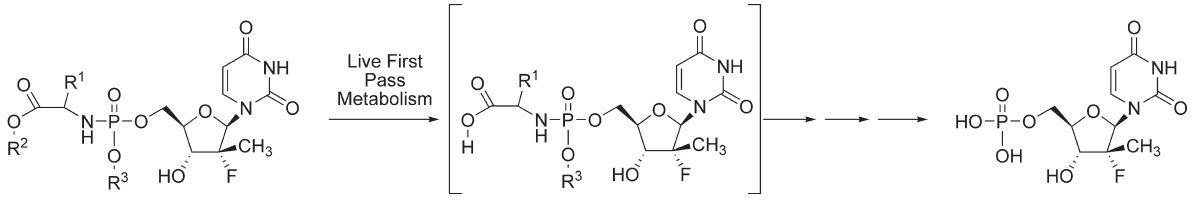

Figure 3. First pass metabolism of the phosphoramidate prodrug derivative of the monophosphate of **5** releases the monophosphate in the liver at the desired site of action.

Scheme 1[a]

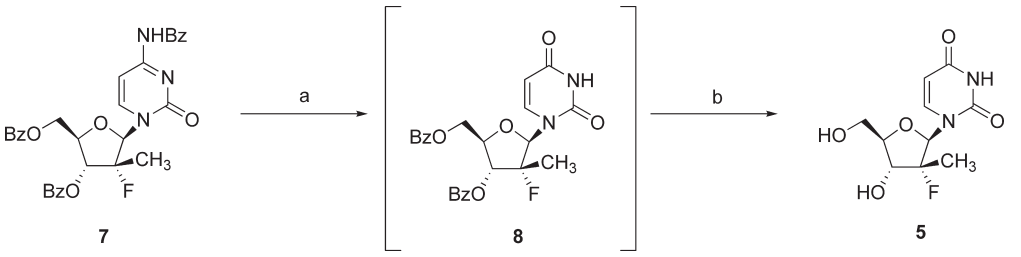

[a] (a) 70% aqueous acetic acid, 100 °C; (b) 25% methanolic ammonia, 0−15 °C.

Scheme 2[a]

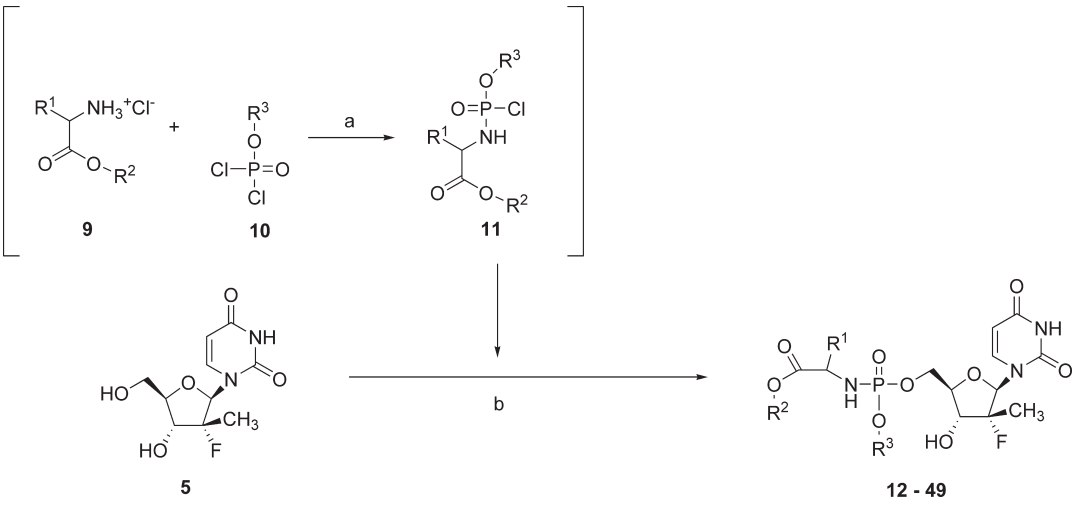

[a] NMI, DCM, −5 to 5 °C; (b) NMI, DCM, 5−25 °C.

ester of the phosphoramidate moiety triggering a cascade of chemical and enzymatic events that would produce the desired uridine monophosphate at the desired site of action, the liver. Subsequently, several reports demonstrated that phosphoramidates of several other anti-HCV nucleosides were able to improve potency, but these reports did not translate this improved in vitro potency into a clinical development candidate.[23−25] Here we describe the discovery of phosphoramidate prodrugs of 2′-deoxy-2′-α-F-2′-*β*-*C*-methyluridine 5′-monophosphate and the selection of **14** and ultimately of its single isomer **51** as clinical development candidates.

Results and Discussion

The development of phosphoramidate prodrugs of **5** began with the investigation of the anti-HCV SAR around the phosphoramidate portion of the molecule. The synthesis of the 2′-deoxy-2′-α-F-2′-*β*-*C*-methyluridine phosphoramidates began with the preparation of the uridine nucleoside **5**. To obtain the uridine nucleoside **5**, we started with the benzoyl protected 2′-deoxy-2′-α-F-2′-*β*-*C*-methylcytidine (**7**). We recently reported on the efficient synthesis of **7**.[26] From **7**, preparation of the uridine nucleoside was efficiently accomplished by a two-step process (Scheme 1). The benzoyl cytidine **7** was heated with 80% acetic acid overnight to afford the protected uridine **8**, which was then treated at room temperature with methanolic ammonia to provide **5** in 78% yield.

The phosphoramidate derivatives of the uridine nucleoside were prepared as shown in Scheme 2. The phosphoramidate moiety was appended by reacting **5** with a freshly prepared chlorophosphoramidate reagent **11** in the presence of NMI.[20] Each chlorophosphoramidate reagent was prepared by stirring an amino acid ester **9** with the appropriate phosphorodichloridate reagent **10** in the presence of an amine base (Et_3N or NMI) in either THF or dichloromethane. The reaction provided the desired 5′-phosphoramidates **12**−**49** as the major product with lesser amounts of the 3′- and 3′,5′-phosphoramidate derivatives. The desired 5′-phosphoramidates were purified by chromatography as a 1:1 mixture of diastereomers at the phosphorus center.

The anti-HCV activity of these prodrugs was assessed using the clone A replicon and a quantitative real time PCR assay.[12] Each compound was simultaneously evaluated for cytotoxicity by assessing for the levels of cellular rRNA.[12] The objective was to identify phosphoramidate prodrugs that exhibited submicromolar activity with the hope that this increased activity would translate into reduced drug load in the clinic relative to **1**. A survey of the terminal carboxylic acid ester of the phosphoramidate moiety in which the amino acid was alanine and the phosphate ester was simply phenyl showed that small simple alkyl and branched alkyl groups provided the desired submicromolar activity; however, in the case of the *n*-butyl (**15**), 2-butyl (**16**), and *n*-pentyl (**17**) esters, cytotoxicity was observed (Table 1). Small cycloalkyl (**18**) and benzyl (**22**, **23**) esters were also compatible; however, phenyl (**21**) and halogenated alkyl groups (**19**, **20**) did not provide the desired potency enhancement.

A survey of the phosphoramidate phosphate ester substituent (Table 2) demonstrated that the 1-naphthyl ester **29**

Table 1. HCV Replicon Activity of Phosphoramidate Prodrugs **12**−**23**: Modification of the Phosphoramidate Ester Moiety

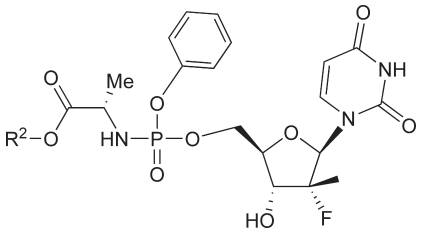

compd	R^2	EC_{90} cloneA (μM)[a]	inhibition of cellular rRNA replication at 50 μM (%)[b]
1		3.9	0
12	Me	0.91	0
13	Et	0.98	36.9
14	*i*-Pr	0.52	25.9
15	*n*-Bu	0.09	79.6
16	2-Bu	0.06	93.8
17	*n*-Pen	>50	92
18	*c*-Hex	0.25	61
19	FCH_2CH_2	1.72	43.8
20	F_2CHCH_2	6.80	38.3
21	Ph	18.50	0
22	Bn	0.13	74.3
23	4-F-Bn	0.24	0

[a] Each value is a result of $n = 2$ determinations. [b] Clone A cells.

Table 2. HCV Replicon Activity of Phosphoramidate Prodrugs **12** and **24**−**30**: Modification of the Phosphoramidate Phenolic Ester Substituent

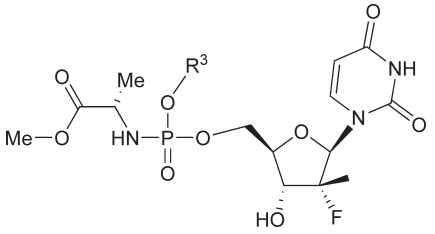

compd	R^3	EC_{90} cloneA (μM)[a]	inhibition of cellular rRNA replication at 50 μM (%)[b]
12	Ph	0.91	0.0
24	4-F-Ph	0.69	16.8
25	4-Cl-Ph	0.58	62.8
26	4-Br-Ph	2.11	30.8
27	3,4-Cl-Ph	0.45	63.7
28	2,4-Cl-Ph	0.69	10.9
29	1-Napth	0.09	95.4
30	Et	>50	16.8

[a] Each value is a result of $n = 2$ determinations. [b] Clone A cells.

provided the greatest potency and that mono- and dihalogenated phenolic esters also gave inhibitors with submicromolar potency. The derivative with a simple alkyl phosphate ester (**30**) was not active against HCV. Although the 1-naphthol ester substitution produced the most potent HCV inhibitor, this substitution also led to substantial cytotoxicity and was therefore not considered a viable substituent.

Study of the amino acid side chain demonstrated that a small alkyl group (**12**, **32**) was accommodated, but α-substitution larger than ethyl showed substantial reduction in potency (Table 3). α-Disubstituted amino acids that included an α-cyclopropanylamino acid derivative **39** did not provide the target submicromolar potency (Table 4). Additionally, it was shown that the natural L-amino acid was required for activity, since the D-alanine derivative **40** was inactive (Table 4).

Results of the phosphoramidate moiety single substituent modifications showed that L-alanine was the preferred amino acid moiety, that methyl, ethyl, isopropyl, or cyclohexyl carboxylate esters provided the desired potency enhancement, and that the phosphate ester accommodated simple phenyl or halogenated phenyl substituents. Subsequently, select combinations of these preferred substitutions were prepared in which only the phenyl or para-halogenated phenyl phosphate ester analogues were examined. Polyhalogenated phosphate esters were excluded from further evaluation in order to preempt any potential toxicity issues that may arise from the release of polyhalogenated phenols upon conversion of the phosphoramidate to the desired nucleoside monophosphate (Table 5).[27−29] The most dramatic difference observed in the SAR for the phosphoramidate substituent combinations was associated with the terminal carboxylic acid ester substituent where the cyclohexyl ester derivatives (**18**, **47**−**49**) showed as much as a 10-fold improvement in potency relative to their methyl, ethyl, or isopropyl analogues. On the basis of replicon potency, initial cytotoxicity profile, and structural diversity,

Table 3. HCV Replicon Activity of Phosphoramidate Prodrugs **12** and **31**−**37**: Modification of the Amino Acid Side Chain

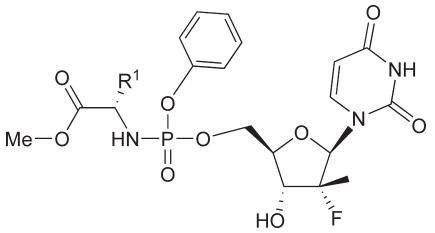

compd	R^1	EC_{90} clone A (μM)[a]	inhibition of cellular rRNA replication at 50 μM (%)[b]
31	H	22.11	0.0
12	Me	0.91	0.0
32	Et	1.61	0.0
33	Me_2CH	>50	0.0
34	Me_2CHCH_2	5.4	0.0
35	$MeSCH_2CH_2$	60.13	24.1
36	$PhCH_2$	57.65	20.6
37	indole-3-CH_2	15.6	68.4

[a] Each value is a result of $n = 2$ determinations. [b] Clone A cells.

Table 4. HCV Replicon Activity of Phosphoramidate Prodrugs **24** and **38**−**40**: α-Disubstituted Amino Acid Side Chains

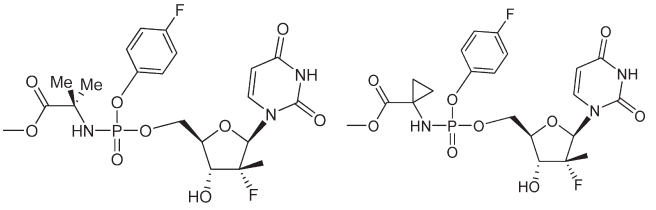

38 **39**

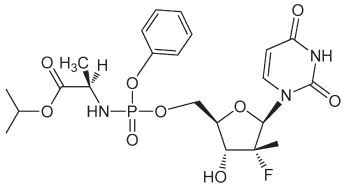

40

compd	EC_{90} clone A (μM)[a]	inhibition of cellular rRNA replication at 50 μM (%)[b]
24	0.69	16.8
38	2.20	0.0
39	>50	0.0
40	>50	0.09

[a] Each value is a result of $n = 2$ determinations. [b] Clone A cells.

a select set of seven compounds (**12**, **14**, **18**, **41**, **44**, **45**, and **47**) was chosen for further evaluation.

To achieve the objective of identifying a phosphoramidate prodrug of the 2′-α-F-2′-β-*C*-methyluridine monophosphate suitable for clinical studies as a treatment for HCV, the prodrug moiety would need to survive exposure in the gastrointestinal tract and preferentially release the nucleotide monophosphate in the liver. Consequently, compounds **12**, **14**, **18**, **41**, **44**, **45**, and **47** were further evaluated for gastrointestinal stability using simulated gastric fluid (SGF) and simulated intestinal fluid (SIF). In addition, stability in human plasma and stability on exposure to human liver S9 fraction were also evaluated (Table 6). The human liver S9 fraction was chosen as a surrogate in vitro model to test for liver stability. The ultimate objective was to select compounds that showed improved potency relative to **4** in the HCV replicon and stability in SGF, SIF, and plasma but showed a short half-life in liver S9, which could indicate rapid release in hepatocytes. Table 6 shows the in vitro stability data for the key compounds selected from combinations of the preferred phosphoramidate substituents. Each of these compounds exhibited prolonged stability ($t_{1/2} > 15$ h) in SGF, SIF, and human plasma but decomposed quickly to the monophosphate when incubated with human liver S9 fraction.

Having the desired target activity and stability profile, compounds **12**, **14**, **18**, **41**, **44**, **45**, and **47** were evaluated in vivo to determine liver levels of the active uridine triphosphate **6** after oral administration. Since HCV replicates in liver cells, measurable levels of nucleoside triphosphate (NTP) should be a strong indication of in vivo efficacy, the assumption being

Table 5. HCV Replicon Activity of Phosphoramidate Prodrugs: Simultaneous Carboxylate and Phenolic Ester Modification of the Phosphoramidate Moiety

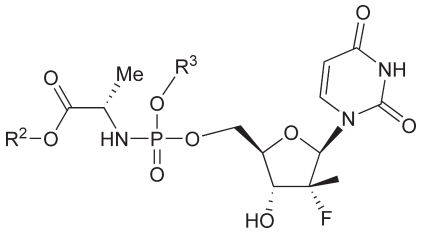

compd	R^2	R^3	EC_{90} cloneA (μM)[a]	inhibition of cellular rRNA replication at 50 μM (%)[b]
12	Me	Ph	1.62	0.0
24	Me	4-F-Ph	0.69	16.8
25	Me	4-Cl-Ph	0.58	62.8
26	Me	4-Br-Ph	2.11	30.8
13	Et	Ph	0.98	36.9
41	Et	4-F-Ph	0.76	55.3
42	Et	4-Cl-Ph	0.39	0.0
43	Et	4-Br-Ph	0.36	80.5
14	*i*-Pr	Ph	0.52	25.9
44	*i*-Pr	4-F-Ph	0.77	0.0
45	*i*-Pr	4-Cl-Ph	0.42	0.0
46	*i*-Pr	4-Br-Ph	0.57	0.0
18	*c*-Hex	Ph	0.25	61.1
47	*c*-Hex	4-F-Ph	0.04	52.1
48	*c*-Hex	4-Cl-Ph	0.054	66.9
49	*c*-Hex	4-Br-Ph	0.039	91.5

[a] Each value is a result of $n = 2$ determinations. [b] Clone A cells.

Table 6. Stability Assessment in SGF, SIF, Human Plasma, and Human Liver S9 Fraction for Compounds **12**, **14**, **18**, **41**, **44**, **45**, and **47**

	stability $t_{1/2}$ (h)			
compd	SGF[a]	SIF[b]	human plasma[c]	human S9[d]
12	15.5	>20	16.7	0.18
14	22	>24	>24	0.57
18	17	>20	>24	1.4
41	17	>20	>8	0.23
44	>20	>20	>24	0.42
45	>20	>20	>24	0.35
47	20	>20	>24	0.18

[a] SGF = simulated gastric fluid, pH 1.2, 50 μg/mL concentration, 37 °C, 20 h. [b] SIF = simulated intestinal fluid, pH 7.5, 50 μg/mL concentration, 37 °C, 20 h. [c] 100 μM, 37 °C, 24 h. [d] 100 μM, 37 °C, 24 h, pH 7.4.

Table 7. PK Parameters of Uridine Triphosphate **6** in Rat Liver after an Oral Dose of 50 mg/kg Phosphoramidate Prodrugs **12**, **14**, **18**, **41**, **44**, **45**, and **47**[a]

compd	C_{max} (ng/g)	t_{max} (h)	AUC(0−t) (ng·h/g)	AUC(inf) (ng·h/g)
12	1985	6.00	14206	18968
14	1934	4.00	16796	18080
18	557	2.00	6487	8831
41	291	4.00	4191	5423
44	519	6.00	6140	7375
45	339	1.00	5143	8468
47	716	4.00	8937	9888

[a] Livers were removed at time points 0.5, 1, 2, 4, 6, and 12 h postdose.

the larger the amount of NTP, the greater the potential efficacy. Therefore, each of the seven key compounds was evaluated in a screening rat PK study where each compound was administered as a single 50 mg/kg oral dose, livers were removed, and liver extracts were assayed for levels of the 2′-deoxy-2′-α-F-2′-*β*-*C*-methyluridine triphosphate. The relative levels of triphosphate found in the liver samples would be an indication of anticipated in vivo potency and would be used to select which of the key compounds would progress further. Table 7 shows the PK parameters for each of the key compounds. Among the seven compounds, compounds **12**, **14**, and **47** produced the highest C_{max} and AUC values. These results strongly suggest that each of these compounds was able to traverse the GI tract, remain intact during the absorption phase, and arrive intact at the target organ, ultimately resulting in high drug exposure in the liver.

Since little is known about which species is predictive of human exposure for nucleoside phosphoramidates, additional in vivo PK assessment was undertaken in dog and cynomolgus monkeys to provide a cross-species comparison of liver exposure to determine whether a dramatic species difference in PK behavior existed among compounds **12**, **14**, and **47**. Comparison of the in vivo PK characteristic in dogs and cynomolgus monkeys was accomplished by evaluating both plasma and liver exposures upon oral q.d. dosing over 4 days with a 50 mg/kg daily dose. Plasma samples were taken on day 3, and liver samples were taken on day 4. Liver levels were determined at a single time point 4 h postdose on day 4 and therefore reflect a single concentration at a single point in time. Plasma and liver levels of phosphoramidate prodrug and liver triphosphate levels were analyzed by LC/MS/MS. In the dog study, compound **14** showed a 16- and 110-fold higher overall plasma exposure (AUC) of the parent prodrug than compounds **12** and **47**, respectively (Table 8). In the monkey compound **14** also provided greater (>3-fold) plasma exposure than did compounds **12** and **47** (Table 9). Similarly, liver exposures in dog and monkey of the parent prodrugs were higher for compound **14** than for compounds **12** and **47**. Triphosphate levels in the liver demonstrated the same relative trends. In dog and monkey compound **14** produced higher triphosphate levels relative to compounds **12** and **47**.

Table 8. Dog Plasma and Liver PK Profile after Oral Administration of Compounds **12**, **14**, and **47**

	plasma (prodrug)[b]					liver[c]	
compd[a]	dose (mg/kg)	C_{max} (ng/mL)	T_{max} (h)	AUC(inf) (ng·h/mL)	AUC(0−t) (ng·h/mL)	prodrug (ng/g liver)	uridine triphosphate **6** (ng/g liver)
12	50	317	1.00	420	418	5.24	4960
14	50	6179	0.50	6903	6894	612	10560
47	50	36	0.25	62	54	8.72	476

[a] Dose of 50 mg/kg for 4 consecutive days. [b] Blood samples collected at 1, 2, 4, 6, 12, and 24 h postdose on day 3. [c] Livers removed at 4 h time point postdose on day 4.

Table 9. Cynomolgus Monkey Plasma and Liver PK Profile after Oral Administration of Compounds **12**, **14**, and **47**

	plasma (prodrug)[b]					liver[c]	
compd[a]	dose (mg/kg)	C_{max} (ng/mL)	T_{max} (h)	AUC(inf) (ng·h/mL)	AUC(0−t) (ng·h/mL)	prodrug (ng/g liver)	uridine triphosphate **6** (ng/g liver)
12	50	19	0.25	34	27	4.66	26
14	50	33	1.00	170	86	177	57
47	50	1.8	6.00	NA	NA	13	NA

[a] Dose of 50 mg/kg for 4 consecutive days. [b] Blood samples collected at 1, 2, 4, 6, 12, and 24 h postdose on day 3. [c] Livers removed at 4 h time point postdose on day 4.

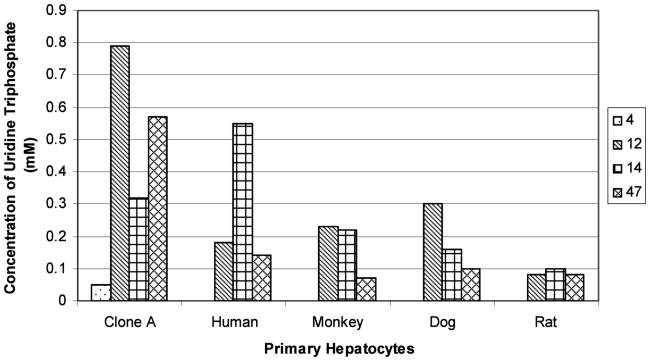

Figure 4. Uridine triphosphate (**6**) levels in human, rat, dog, and monkey primary hepatocytes when treated with **4** and uridine phosphoramidates **12**, **14**, and **47**.

However, it should be noted that the liver triphosphate data were only used for an intraspecies comparison of compounds. One should not compare the relative dog to monkey liver triphosphate levels because of the liver single time point sampling protocol.

Since the generation of triphosphate levels is critical to predicting in vivo potency of nucleos(t)ide analogues, in vitro triphosphate production in primary human hepatocytes was examined and compared to in vitro triphosphate levels determined in primary hepatocytes from rat, dog, and monkey when incubated with compounds **12**, **14**, and **47**. An analysis of uridine triphosphate (**6**) production in these primary hepatocyte studies would provide a comparison of the inherent capacity of each nucleotide phosphoramidate to both enter hepatocytes and be converted to the target triphosphate. In vitro analysis of triphosphate production was accomplished by incubating each compound for 48 h with primary hepatocytes from rat, dog, monkey, and human and then extracting the cells and analyzing the extracts by HPLC.[19,30] The triphosphate levels generated in the primary hepatocytes were compared to triphosphate levels generated in clone A replicon cells and to the triphosphate levels generated on exposure to a known clinically efficacious agent, **4**. Figure 4 shows that for compounds **12**, **14**, and **47** 2′-F,2′-*C*-methyluridine 5′-triphosphate levels in clone A cells were 6- to 16-fold greater than 2′-F,2′-*C*-methylcytidine 5′-triphosphate levels generated by cells when incubated with cytidine nucleoside **4**. These enhanced triphosphate levels in clone A cells are consistent with the increased potency observed for compounds **12**, **14**, and **47** when compared to **4**. 2′-F,2′-*C*-methyluridine 5′-triphosphate levels in primary hepatocytes of human, rat, dog, and monkey incubated with compounds **12**, **14**, and **47** were also shown to be high, whereas in each case the triphosphate levels following incubation with **4** were shown to be below the limit of detection. Compound **47** consistently showed the lowest triphosphate levels of the three phosphoramidate analogues. Compound **14** demonstrated 3- to 4-fold higher triphosphate levels in human primary hepatocytes relative to compounds **12** and **47**. Compounds **12** and **14** produced comparable amounts of triphosphate in monkey and rat hepatocytes, whereas in dog hepatocytes compound **12** showed 2-fold higher levels than **14**. The interspecies differences observed regarding conversion of phosphoramidates **12**, **14**, and **47** to the active triphosphate **6** may be attributed to either cross-species differences in the level of enzymes needed to convert the phosphoramidates to the intermediate monophosphate or to differences in cell penetration. Similarly, since each of the phosphoramidates **12**, **14**, and **47** is converted to the same triphosphate metabolite, intraspecies differences could be attributed to the selectivity of processing enzymes or to the ability to penetrate the species specific hepatocytes by each of the different analogues. To assess relative membrane permeability characteristics, both calculated AlogP values and parallel artificial membrane permeability (PAMPA) were evaluated. Both AlogP and PAMPA results indicate that the predicted order of cell permeability would be **47** > **14** > **12**, in line with lipophilic character (Table 10).[31,32] This relative order tracks well with the relative replicon EC_{90} values; however, the order does not necessarily correlate to triphosphate levels observed in hepatocytes. Therefore, it is possible that other factors such as

Table 10. AlogP and PAMPA Profile of Compounds **12**, **14**, and **47**

compd	AlogP[a]	PAMPA permeability (nm/s)[b]
12	0.19	0.07
14	0.92	0.46
47	2.26	4.88

[a] Reference 31. [b] pH 7.4, incubated for 12−24 h.

selectivity for processing enzymes or relative levels of processing enzymes in hepatocytes from different species are contributing to the relative difference in cellular triphosphate levels observed.

Nucleos(t)ide toxicity can be correlated to several cellular effects. Mitochondrial toxicity has been reported to be associated with the long-term use of certain nucleos(t)ide analogues resulting in myopathy, peripheral neuropathy, and pancreatitis.[33,34] Hematotoxicity, which can lead to neutropenia, severe anemia, and thrombocytopenia, has also been associated with several nucleoside analogues including the HCV polymerase inhibitor **3**.[35,36] One cause of hematotoxicity is bone marrow toxicity.[35,36] To examine for these possible toxicities, compounds **12**, **14**, and **47** were evaluated for general cytotoxicity against an expanded cell panel and evaluated in vitro for both mitochondrial toxicity and toxicity to bone marrow progenitor cells. In an expanded cell panel that included two human hepatocyte cell lines, Huh7 and HepG2, a human pancreatic cell line, BxBC3, and a human T lymphoblast cell line, CEM, compounds **12**, **14**, and **47** were found to show no cytotoxicity up to 100 μM, the highest concentration tested. Compounds **12**, **14**, and **47** were assessed for mitochondrial toxicity in both CEM and HepG2 cells by incubating each compound for 14 days. Percentage inhibition of mitochondrial DNA production was determined relative to a no drug control. No inhibition of mitochondrial DNA synthesis up to the highest concentration tested (50 μM) was observed for the three compounds. To evaluate the potential for bone marrow toxicity, compounds **12**, **14**, and **47** were screened from 0.1 to 50 μM for their effect on human erythroid and myeloid progenitor cell colony proliferation. Differentiation of hematopoietic progenitors into erythroid or granulocyte-myeloid cell lineages over 14 days was measured. The results showed that compounds **12** and **14** had IC_{50} values of >50 μM for both erythroid and myeloid progenitor cells. Erythroid and myeloid progenitor cells were more sensitive to compound **47** which showed IC_{50} values of 37 $\pm$ 5 μM and 30 $\pm$ 5 μM for erythroid and myeloid progenitor cells, respectively. Since each phosphoramidate derivative leads to the same metabolic intermediates, it is unlikely that the metabolic intermediates leading to the triphosphate active metabolite contribute to the effects on erythroid or myeloid progenitor cells. Therefore, since the only difference between compounds **12**, **14**, and **47** resides in the nature of the carboxylic acid ester and the phenolic ester substituents, it would appear that the character of the carboxylate and/or phenolic esters contributes significantly to the effect on erythroid and myeloid progenitor cells and therefore the potential for bone marrow toxicity. The effect on progenitor cells observed for compound **47** could be a result of the phosphoramidate itself or from the released ester moieties after prodrug metabolism.

A comparison of in vivo acute toxicity of compounds **12**, **14**, and **47** was undertaken by single dose oral administration in rats with a 14-day postdose observation period. Rats (three males and three females) were dosed with each compound at doses of 50, 300, and 1800 mg/kg. Fourteen days after dose administration, all rats were euthanized and daily clinical observations, body weights, macroscopic pathology including kidney and liver weights were assessed. For each of the compounds, no test-article-related mortality, clinical signs of toxicity, body weight changes, macroscopic pathology, or organ weight changes for liver and kidney were observed in any of the treatment groups. Consequently, for each of the compounds studied the NOAEL was established at >1800 mg/kg.

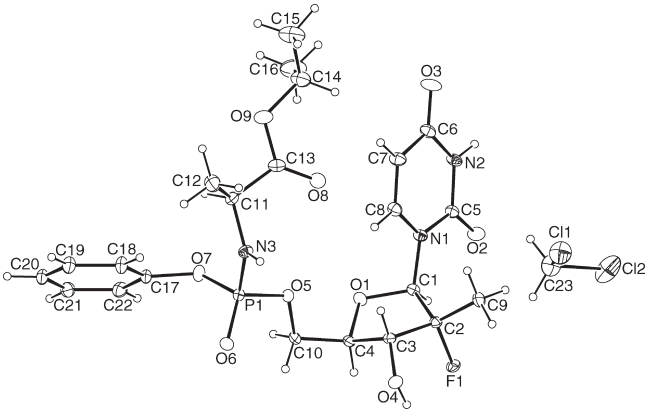

Figure 5. X-ray crystal structure of **51** crystallized from CH_2Cl_2.

In vitro hepatocyte triphosphate levels and in vivo PK profiles and effects on bone marrow progenitor cells were factors that differentiated compounds **12**, **14**, and **47**. Compound **14** consistently produced high levels of triphosphate across all species and in particular showed the greatest triphosphate levels in primary human hepatocytes by as much as 3-fold over compounds **12** and **47**. The in vivo PK assessment showed that compound **14** consistently demonstrated the highest liver triphosphate levels across species. Bone marrow toxicity studies showed that no difference in safety profile was observed between compounds **12** and **14**; however, bone marrow progenitor cells were more sensitive to the presence of compound **47**. On the basis of the overall profile, compound **14** (PSI-7851) was selected for further development.[37]

14 is a 1:1 mixture of diastereomers at the phosphorus center of the phosphoramidate moiety and is a low melting point (mp = 66−75 °C) amorphous solid. The diastereomers of **14** were separated by HPLC chromatography to give the two pure diastereomers **50** (fast moving isomer) and **51** (slow moving isomer). In the clone A replicon assay, compounds **50** and **51** produced anti-HCV activity with EC_{90} values of 7.5 and 0.42 μM, respectively, thus demonstrating a >10-fold difference in activity between the two isomers. Diastereomer **51** was subsequently crystallized using methylene chloride as the solvent, and a single crystal X-ray structure of **51** was obtained, definitively establishing the configuration of the phosphorus center as *S*p and by corollary the configuration of **50** as *R*p (Figures 5 and 6). This is the first demonstrated crystallization and X-ray structure determination of a phosphoramidate nucleotide prodrug and the first example where stereochemistry at phosphorus could be correlated unequivocally to nucleotide phosphoramidate activity.

Each diastereomer was also evaluated against replicons containing known nucleoside resistant mutations. The S282T NS5B polymerase mutation was shown to afford a low level of resistance to the 2′-deoxy-2′-α-F-2′-*β*-*C*-methylcytidine nucleoside **4**, and the S96T mutation was shown to afford resistance to the 4′-azidocytidine nucleoside **3**.[38−40] The individual uridine phosphoramidate isomers **50** and **51** were evaluated against these known nucleoside resistant mutants, and as expected, the S282T mutant was resistant to both isomers **50** and **51** with EC_{90} fold increases of >13 and 18.6, respectively. No cross-resistance was observed when each isomer was tested against the S96T mutation (Table 11).

Diastereoisomers **50** and **51** were evaluated for their ability to generate intracellular levels of the active uridine triphosphate **6** in clone A and primary human hepatocytes.[19,30]

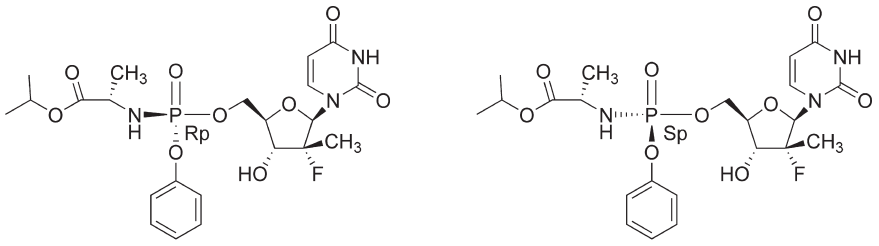

50 (PSI-7976) **51** (PSI-7977)

Figure 6. Structures of diastereomers **50** and **51**.

Table 11. Cross-Resistance Studies Using Replicon Mutants (S282T and S96T/N142T) Resistant to Nucleotide Inhibitors **50** and **51**

	clone A: EC_{90} (μM)[a]		EC_{90} fold increase[b]	ET-lunet: EC_{90} (μM)[a]		EC_{90} fold increase[b]
compd[c]	WT	S282T	S282T/WT	WT	S96T	S96T/WT
50	7.5 ± 3.0	>100	>13	3.3 ± 1.4	1.3 ± 0.3	0.4
51	0.42 ± 0.23	7.8 ± 5.3	18.6	0.23 ± 0.15	0.11 ± 0.039	0.5

[a] Increasing concentrations of **50** or **51** were added to wild type (WT), S282T, or S96T/N142T replicon cells (clone A or ET-lunet). The concentration at which 90% inhibition (EC_{90}) occurred was calculated. [b] The fold change in EC_{90} of the inhibitor against the S282T or S96T/N142T mutant replicon compared to the wild type replicon was determined. [c] At least three independent experiments were performed for the compounds in each cell line.

When clone A cells were incubated for 24 h in the presence of **50** or **51** (5 μM), diastereoisomer **51** produced 29.3 μM of triphosphate while compound **50** produced only 2.7 μM, a 10-fold difference in favor of **51**. When incubated with primary human hepatocytes under the same conditions, the level of triphosphate produced with diastereomer **51** (45.0 μM) was 14% greater than that produced with diastereomer **50** (39.5 μM). It is interesting to note that the overall levels of triphosphate produced in human hepatocytes is significantly greater than seen in clone A replicon cell line. In addition, it is clear that there is a diastereomer preference for triphosphate formation favoring diastereomer **51** over **50**.

Comparison of cytotoxicity profiles for each isomer (**50** and **51**) demonstrated that both compounds were essentially devoid of cytotoxicity when assessed in an 8-day cytotoxicity assay against an expanded cell panel (Huh7, HepG2, BxPC3, and CEM cells) at concentrations up to 100 μM. When mitochondrial toxicity (CC_{90}) was evaluated by incubating CEM and HepG2 cells with compounds **50** and **51** for 14 days and then measuring the levels of mitochondrial COXII DNA (mtDNA) and ribosomal DNA (rDNA) using real time PCR, both compounds demonstrated no measurable mitochondrial toxicity up to 100 μM in CEM cells but compound **51** showed a CC_{90} of 72.1 and 68.6 μM for the inhibition of mtDNA and rDNA, respectively, in HepG2 cells.

On the basis of its superior potency and ability to produce higher intracellular triphosphate levels, diastereomer **51** was selected as the preferred diastereomer for further study. Subsequently, we have applied the above crystallization conditions to selectively crystallize the more active diastereomer **51** from the diastereomeric mixture **14**. These crystallization conditions have been applied on multikilogram scale to support further development of **51**. The uridine phosphoramidate **51** (PSI-7977) is currently in phase II clinical trials for the treatment of HCV infection.[37]

Conclusion

We have demonstrated that application of the phosphoramidate prodrug approach to the 5′-monophosphate of 2′-deoxy-2′-α-F-2′-*β*-*C*-methyluridine produced nucleotide derivatives with potent anti-HCV activity and that these phosphoramidates were effective at delivering high levels of active triphosphate both in vitro and in vivo. **14** was selected as a development candidate and demonstrated early clinical proof of concept for the treatment of HCV infection by a 2′-α-F-2′-*β*-*C*-methyluridine phosphoramidate. Identification of **51** as the preferred single diastereomer resulted in the first crystallization and X-ray structure determination of a nucleotide phosphoramidate and correlation of phosphoramidate stereochemistry with biological potency. The *S*p diastereomer **51** is currently in phase II clinical development for the treatment of HCV infection.

Experimental Section

Nuclear magnetic resonance (NMR) spectra were recorded on a Bruker advance II 400 MHz and a Varian Unity Plus 400 MHz spectrometers at room temperature, with tetramethylsilane as an internal standard. Chemical shifts (δ) are reported in parts per million (ppm), and signals are reported as s (singlet), d (doublet), t (triplet), q (quartet), m (multiplet), or br s (broad singlet). Purities of the final compounds were determined by HPLC and were greater 95%. HPLC conditions to assess purity were as follows: Shimadzu HPLC 20AB Sepax HP-C18 4.6 mm × 50 mm (5 μm); flow rate, 3.0 mL/min; acquire time, 6 min; wavelength, UV 220 nm; oven temperature, 40 °C. Chiral HPLC was conducted on Shimadzu HPLC 20A. The preparative HPLC system includes two sets of Gilson 306 pumps, a Gilson 156 UV/vis detector, and a Gilson 215 injector and fraction collector, with Unipoint control software. A YMC 25 mm × 30 mm × 2 mm column was used. The mobile phase was HPLC grade water (A) and HPLC grade acetonitrile (B) system. SFC was conducted on Berger Multi-Gram SFC from Mettler Toledo Co, Ltd. LC/MS was conducted on Shimadzu LCMS 2010EV using electrospray positive [ES+ve to give MH^+] equipped with a Shim-pack XR-ODS 2.2 μm column (3.0 mm × 30 mm, 3.0 mm i.d.), eluting with 0.0375% TFA in water (solvent A) and 0.01875% TFA in acetonitrile (solvent B). High-resolution mass spectra were obtained on a Agilent G1969a spectrometer.

2′-Deoxy-2′-fluoro-2′-C-methyluridine (5). 3′,5′-*O*-Dibenozyl-2′-deoxy-2′-fluoro-2′-*C*-methyl-*N*4-benzoylcytidine (**7**, 500 g, 0.874 mol) was added to 70% aqueous acetic acid (7.5 L). The solution was heated to reflux (110 °C) for 20 h. The mixture was cooled to ambient temperature and diluted with water (2 L). After the mixture was stirred for 2 h, the resulting precipitate

was collected by filtration and the solid was rinsed with water (5 L) and dried in the atmosphere at ambient temperature for 12 h to afford 360 g (88%) of the dibenzoyluridine intermediate **8**. This in turn was used as is in the next step by adding it all to freshly prepared 25% methanolic ammonia (5.4 L) at 0 °C. This temperature was maintained for 3 h and then allowed to warm to 15 °C for 24 h. The reaction mixture was filtered through a Celite bed and concentrated under reduced pressure to give the crude product (216 g). The crude product was stirred with ethyl acetate (325 mL) for 3 h at ambient temperature. The resulting solid was collected by filtration and washed with ethyl acetate (200 mL). The solid was dried under vacuum at ambient temperature for 4 h to afford 160 g (78%) of the desired product **5** in 98.7% HPLC purity. ^{1}H NMR (DMSO-d_6) d 11.44 (br s, 1H, NH), 7.95 (d, 1H, C-6H), 5.97 (d, 1H, C-1′H), 5.64 (d, 1H, C-5H), 3.84−3.77 (m, 3H, C-5′-Ha, C-3′H, C-4′H), 3.63−3.60 (m, 1H, C5′-Hb), 1.23 (d, 3H, C-2′-CH_3). ES-MS M − 1, 259.

General Procedure for the Preparation of Compounds 12−49. Preparation of Intermediates 11. To a solution of compound **10**[1] (5 mmol) and compound **9** (5 mmol) in dichloromethane (25 mL), triethylamine or *N*-methylimidazole (1 g, 10 mmol) in anhydrous dichloromethane (25 mL) was added dropwise with vigorous stirring at −78 or −5 °C over a period of 2 h. The mixture was allowed to warm to 5 °C or room temperature gradually and stirred for an additional 0.5 h. Solvent was evaporated under reduced pressure, and the residue was treated with anhydrous ether (20 mL). The precipitated triethylammonium chloride salt was filtered and washed with ether (10 mL). Solvent was evaporated from the combined filtrate to give the crude product **11** as colorless oil, and they were used in the next step without further purification.

Preparation of Products 12−49. To a well-stirred mixture of 2′-deoxy-2′-fluoro-2′-*C*-methyluridine (**5**, 0.15 g,1 equiv) and *N*-methylimidazole (0.3 g, 8 equiv) in THF (3 mL) at room temperature, the phosphorochloridate intermediate (**11**, 6.5 equiv) in THF (3 mL) was added in one lot and the mixture was vigorously stirred at room temperature overnight. Solvent was evaporated under reduced pressure. The resulting crude product was dissolved in methanol and purified by preparative HPLC on a YMC 25 mm × 30 mm × 2 mm column using a water/acetonitrile gradient elution mobile phase. The acetonitrile and water were removed under reduced pressure to give the desired product. The final products were characterized by LC/MS and ^{1}H NMR.

(*S*)-2-{[(2*R*,3*R*,4*R*,5*R*)-5-(2,4-Dioxo-3,4-dihydro-2*H*-pyrimidin-1-yl)-4-fluoro-3-hydroxy-4-methyltetrahydrofuran-2-ylmethoxy]-phenoxyphosphorylamino}propionic Acid Methyl Ester (12). Yield: 15.6%. ^{1}H NMR (DMSO-d_6) δ 1.20−1.27 (m, 6H), 3.58 (d, J = 16.0 Hz, 3H), 3.76−3.92 (m, 2H), 4.02−4.38 (m, 2H), 5.54 (t, J = 10.2 Hz, 1H), 5.84−5.91 (m, 1H), 6.00−6.16 (m, 1H), 7.18 (d, J = 8.0 Hz, 2H), 7.22 (s, 1H), 7.35 (t, J = 4.4 Hz, 2H), 7.55 (s, 1H), 11.52 (s, 1H); ^{13}C NMR (DMSO-d_6) δ 174.61, 174.57, 174.51, 174.46, 163.69, 151.60, 151.54, 151.39, 140.27, 130.61, 125.55, 121.04, 120.99, 120.96, 103.26, 103.18, 102.17, 100.37, 89.50, 80.36, 72.34, 65.55, 65.28, 52.82, 50.73, 50.58, 27.77, 20.71, 20.65, 20.58, 20.51, 17.60, 17.35; MS, *m*/*e* 502 (M+1)$^+$. HRMS, calcd for $C_{20}H_{26}FN_3O_9P$ (M^+ + H), 502.1385; found, 502.1372.

(*S*)-2-{[(2*R*,3*R*,4*R*,5*R*)-5-(2,4-Dioxo-3,4-dihydro-2*H*-pyrimidin-1-yl)-4-fluoro-3-hydroxy-4-methyltetrahydrofuran-2-ylmethoxy]-phenoxyphosphorylamino}propionic Acid Ethyl Ester (13). Yield: 19.6%. ^{1}H NMR (DMSO-d_6) δ 1.13−1.16 (m, 3H), 1.20−1.28 (m, 6H), 3.70−3.90 (m, 2H), 4.00−4.08 (m, 3H), 4.18−4.39 (m, 2H), 5.53−5.58 (m, 1H), 5.86−5.98 (m, 1H), 6.01−6.13 (m, 2H), 7.16−7.23 (m, 3H), 7.37−7.40 (m, 2H), 7.54−7.57(m, 1H), 11.54 (s,1H); MS, *m*/*e* 516.1 (M + 1)$^+$. HRMS, calcd for $C_{21}H_{28}FN_3O_9P$ (M^+ + H), 516.1542; found, 516.1526.

(*S*)-2-{[(2*R*,3*R*,4*R*,5*R*)-5-(2,4-Dioxo-3,4-dihydro-2*H*-pyrimidin-1-yl)-4-fluoro-3-hydroxy-4-methyltetrahydrofuran-2-ylmethoxy]-phenoxyphosphorylamino}propionic Acid Isopropyl Ester (14). Yield: 6%. ^{1}H NMR (DMSO-d_6) δ 1.13−1.28 (m, 12H), 3.75−3.81 (m, 2H), 3.95−4.08 (m,1H), 4.20−4.45 (m, 2H), 4.83−4.86 (m, 1H), 5.53−5.58 (m, 1H), 5.84−6.15 (m, 3H), 7.18−7.23 (m, 3H), 7.35−7.39 (m, 2H), 7.54−7.57 (m, 1H), 11.50 (s, 1H); ^{13}C NMR (DMSO-d_6) δ 173.70, 173.66, 173.59, 173.54, 163.70, 151.60, 151.40, 140.25, 130.63, 125.55, 121.04, 120.99, 120.95, 103.28, 103.21, 102.20, 100.37, 89.42, 80.33, 72.33, 68.98, 68.95, 65.60, 65.14, 50.88, 50.72, 27.79, 22.37, 22.32, 20.77, 20.71, 20.64, 20.57, 17.60, 17.36; MS, *m*/*e* 530.2 (M + 1)$^+$. HRMS, calcd for $C_{22}H_{30}FN_3O_9P$ (M^+ + H), 530.1698; found, 530.1685. The two diastereomers were separated using column chromatography on silica gel using 2−5% isopropanol in dichloromethane as the eluent.

(*S*)-2-{(*R*)-[(2*R*,3*R*,4*R*,5*R*)-5-(2,4-Dioxo-3,4-dihydro-2*H*-pyrimidin-1-yl)-4-fluoro-3-hydroxy-4-methyltetrahydrofuran-2-ylmethoxy]phenoxyphosphorylamino}propionic Acid Isopropyl Ester (50). ^{1}H NMR (DMSO-d_6) δ 11.53 (s, 1H), 7.56 (d, J = 8.0 Hz, 1H), 7.39−7.35 (m, 2H), 7.20−7.15 (m, 3H), 6.13−6.07 (m, 1H), 5.91 (d, J = 7.2 Hz, 1H), 5.57 (dd, J = 2.0, 8.0 Hz, 1H), 4.85 (sextet, J = 6.4 Hz, 1H), 4.43−4.38 (m, 1H), 4.30−4.23 (m, 1H), 4.05 (dm, J = 6.4 Hz, 1H), 3.80−3.72 (m, 2H), 1.24 (d, J = 22.4 Hz, 3H), 1.20 (d, J = 6.8 Hz, 3H), 1.15 (dd, J = 2.8, 6.0 Hz, 6H); ^{31}P NMR (DMSO-d_6) δ 4.76; MS (ESI) (M + H)$^+$ 530.1. HRMS, calcd for $C_{22}H_{30}FN_3O_9P$ (M^+ + H), 530.1698; found, 530.1686.

(*S*)-2-{[(1*R*,4*R*,5*R*)-5-(2,4-Dioxo-3,4-dihydro-2*H*-pyrimidin-1-yl)-4-(*R*)-fluoro-3-hydroxy-4-methyltetrahydrofuran-2-yl-methoxy]phenoxyphosphorylamino}propionic Acid (*S*)-Isopropyl Ester (51). ^{1}H NMR (DMSO-d_6) δ 11.50 (s, 1H), 7.54 (d, J = 8.0 Hz, 1H), 7.38−7.33 (m, 2H), 7.21−7.15 (m, 3H), 6.06−5.99 (m, 2H), 5.82 (m, 1H), 5.52 (d, J = 8.0 Hz, 1H), 4.84 (quintet, J = 6.4 Hz, 1H), 4.38−4.32 (m, 1H), 4.23−4.18 (m, 1H), 4.01−3.96 (m, 1H), 3.84−3.72 (m, 2H), 1.24 (d, J = 17.2 Hz, 3H), 1.21 (d, J = 6.4 Hz, 3H), 1.13 (d, J = 6.0 Hz, 6H); ^{31}P NMR (DMSO-d_6) δ 4.89; MS (ESI) (M + H)$^+$ 530.1. HRMS, calcd for $C_{22}H_{30}FN_3O_9P$ (M^+ + H), 530.1698; found, 530.1683.

(*S*)-2-{[(2*R*,3*R*,4*R*,5*R*)-5-(2,4-Dioxo-3,4-dihydro-2*H*-pyrimidin-1-yl)-4-fluoro-3-hydroxy-4-methyltetrahydrofuran-2-ylmethoxy]-phenoxyphosphorylamino}propionic Acid Butyl Ester (15). Yield: 12.7%. ^{1}H NMR (DMSO-d_6) δ 0.81−0.85 (m, 3H), 1.20−1.30 (m, 8H), 1.47−1.51 (m, 2H), 3.78−3.88 (m, 2H), 3.95−4.08 (m, 3H), 4.22−4.45 (m, 2H), 5.56−5.58 (t, 1H), 5.85−6.18 (m, 3H), 7.18−7.23 (m, 3H), 7.37−7.39 (m, 2H), 7.51−7.60 (d, 1H), 11.50 (s.1H); MS, *m*/*e* 544.2 (M + 1)$^+$. HRMS, calcd for $C_{23}H_{32}FN_3O_9P$ (M^+ + H), 544.1855; found, 544.1839.

(*S*)-2-{[(2*R*,3*R*,4*R*,5*R*)-5-(2,4-Dioxo-3,4-dihydro-2*H*-pyrimidin-1-yl)-4-fluoro-3-hydroxy-4-methyltetrahydrofuran-2-ylmethoxy]-phenoxyphosphorylamino}propionic Acid *sec*-Butyl Ester (16). Yield: 6.3%. ^{1}H NMR (DMSO-d_6) δ 0.89 (d, J = 6.8 Hz, 6H), 1.20−1.26 (m, 6H), 1.79−1.86 (m, 1H), 3.37−3.90 (m, 4H), 4.01 (t, J = 11.2 Hz, 1H), 4.21−4.28 (m, 1H), 4.33−4.42 (m, 1H), 5.54 (t, J = 7.6 Hz, 1H), 5.85−5.92 (m, 1H), 5.99−6.13 (m, 2H), 7.19 (t, J = 8 Hz, 3H), 7.36 (t, J = 7.6 Hz, 2H), 7.53 (d, J = 7.6 Hz, 1H), 11.52 (s, 1H); MS, *m*/*e* 544.00 (M + 1)$^+$. HRMS, calcd for $C_{23}H_{32}FN_3O_9P$ (M^+ + H), 544.1855; found, 544.1840.

(*S*)-2-{[(2*R*,3*R*,4*R*,5*R*)-5-(2,4-Dioxo-3,4-dihydro-2*H*-pyrimidin-1-yl)-4-fluoro-3-hydroxy-4-methyltetrahydrofuran-2-ylmethoxy]-phenoxyphosphorylamino}propionic Acid Pentyl Ester (17). Yield: 32.2%. ^{1}H NMR (DMSO-d_6) δ 0.80−0.81 (m, 3H), 1.17−1.23 (m, 10H), 1.47−1.50 (m, 2H), 3.77−3.81 (m, 2H), 3.94−3.96 (m, 3H), 4.21−4.36 (m, 2H), 5.52−5.54 (m, 1H), 5.87−6.01 (m, 3H), 7.14−7.19 (m, 3H), 7.32−7.35 (m, 2H), 7.51 (d, J = 8 Hz, 1H), 11.49 (s, 1H); MS, *m*/*e* 557.9 (M + 1)$^+$; 1136.88 (2M + 23)$^+$. HRMS, calcd for $C_{24}H_{34}FN_3O_9P$ (M^+ + H), 558.2011; found, 558.1998.

(*S*)-2-{[(2*R*,3*R*,4*R*,5*R*)-5-(2,4-Dioxo-3,4-dihydro-2*H*-pyrimidin-1-yl)-4-fluoro-3-hydroxy-4-methyltetrahydrofuran-2-yl-methoxy]phenoxyphosphorylamino}propionic Acid Cyclohexyl Ester (18). Yield: 19.3%. ^{1}H NMR (DMSO-d_6) δ 1.18−1.41 (m, 12H), 1.59−1.67 (m, 4H), 3.74−3.80 (m, 1H), 3.96−4.02 (m, 1H), 4.19−4.26 (m, 1H), 4.31−4.39 (m, 1H), 4.59 (s, 1H), 5.52 (t, J = 7.8 Hz, 1H), 5.80−6.09 (m, 3H), 7.15−7.20 (m, 3H), 7.32−7.36 (m, 2H), 7.52 (d, J = 8 Hz, 1H), 11.50 (s, 1H); ^{13}C NMR

(DMSO-d_6) δ 173.61, 173.57, 173.50, 173.45, 163.68, 151.64, 151.58, 151.40, 140.18, 130.63, 125.55, 121.04, 120.99, 120.95, 103.28, 103.22, 102.19, 100.39, 89.37, 80.37, 73.48, 72.35, 65.15, 50.92, 50.75, 31.80, 31.72, 25.76, 23.94, 20.86, 20.80, 20.73, 20.66, 17.60, 17.35; MS, *m/e* 569.98 $(M + 1)^+$; 592.14 $(M + 23)^+$. HRMS, calcd for $C_{25}H_{34}FN_3O_9P$ $(M^+ + H)$, 570.2011; found, 570.1999.

(*S*)-2-{[(2*R*,3*R*,4*R*,5*R*)-5-(2,4-Dioxo-3,4-dihydro-2*H*-pyrimidin-1-yl)-4-fluoro-3-hydroxy-4-methyltetrahydrofuran-2-ylmethoxy]-phenoxyphosphorylamino}propionic Acid 2-Fluoroethyl Ester (19). Yield: 7%. ^{1}H NMR (DMSO-d_6) δ 1.18−1.25 (m, 6H), 3.71−3.89 (m, 2H), 3.92−3.99 (m, 1H), 4.19−4.27 (m, 4H), 4.48−4.61 (m, 2H), 5.52 (m, 1H), 5.90−6.14 (m, 2H), 7.15−7.21 (m, 3H), 7.32−7.36 (m, 2H), 7.46−7.57 (m, 1H), 11.49 (s,1H); MS, *m/e* 533.86 $(M + 1)^+$. HRMS, calcd for $C_{21}H_{27}F_2N_3O_9P$ $(M^+ + H)$, 534.1447; found, 534.1434.

(*S*)-2-{[(2*R*,3*R*,4*R*,5*R*)-5-(2,4-Dioxo-3,4-dihydro-2*H*-pyrimidin-1-yl)-4-fluoro-3-hydroxy-4-methyltetrahydrofuran-2-ylmethoxy]phenoxyphosphorylamino}propionic Acid 2,2-Difluoroethyl Ester (20). Yield: 7%. ^{1}H NMR (DMSO-d_6) δ 1.17−1.24 (m, 6H), 3.67−3.81 (m, 1H), 3.89−3.98 (m, 2H), 4.21−4.36 (m, 4H), 5.48−5.53 (m, 1H), 5.82−6.05 (m, 2H), 6.18−6.22 (m, 2H), 7.15−7.20 (m, 3H), 7.32−7.36 (m, 2H), 7.51 (s, 1H), 11.50 (s, 1H); MS, *m/e* 551.92 $(M + 1)^+$. HRMS, calcd for $C_{21}H_{26}F_3N_3O_9P$ $(M^+ + H)$, 552.1353; found, 552.1342.

(*S*)-2-{[(2*R*,3*R*,4*R*,5*R*)-5-(2,4-Dioxo-3,4-dihydro-2*H*-pyrimidin-1-yl)-4-fluoro-3-hydroxy-4-methyltetrahydrofuran-2-ylmethoxy]phenoxyphosphorylamino}propionic Acid Phenyl Ester (21). Yield: 21%. ^{1}H NMR (DMSO-d_6) δ 1.19−1.25 (m, 3H), 1.38−1.41 (m, 3H), 3.72−3.91 (m, 1H), 4.04−4.14 (m, 2H), 4.28−4.31 (m, 1H), 4.41−4.43 (m, 1H), 5.49−5.55 (m, 1H), 5.88−6.07 (m, 2H), 6.33−6.36 (m,1H), 7.03−7.06 (m, 2H), 7.16−7.27 (m, 4H), 7. 35−7. 39 (m, 4H), 7.41−7.54 (m, 1H), 11.51 (s, 1H); MS, *m/e* 563.91 $(M + 1)^+$, 1148.82 $(2M + 23)^+$. HRMS, calcd for $C_{25}H_{28}FN_3O_9P$ $(M^+ + H)$, 564.1542; found, 564.1529.

(*S*)-2-{[(2*R*,3*R*,4*R*,5*R*)-5-(2,4-Dioxo-3,4-dihydro-2*H*-pyrimidin-1-yl)-4-fluoro-3-hydroxy-4-methyltetrahydrofuran-2-ylmethoxy]phenoxyphosphorylamino}propionic Acid Benzyl Ester (22). Yield: 12.5%. ^{1}H NMR (DMSO-d_6) δ 1.20−1.28 (m, 6H), 3.72−4.01 (m, 3H), 4.23−4.26 (m, 1H), 4.37−4.38 (m, 1H), 5.08−5.09 (t, 2H), 5.52−5.56 (t, 1H), 5.86−6.04 (m, 2H), 6.16−6.19 (m,1H), 7.15−7.21 (m, 3H), 7.30−7.36 (m, 7H), 7.54−7.56 (d, 1H), 11.50 (s.1H); MS, *m/e* 578.2 $(M + 1)^+$. HRMS, calcd for $C_{26}H_{30}FN_3O_9P$ $(M^+ + H)$, 578.1698; found, 578.1689.

(*S*)-2-{[(2*R*,3*R*,4*R*,5*R*)-5-(2,4-Dioxo-3,4-dihydro-2*H*-pyrimidin-1-yl)-4-fluoro-3-hydroxy-4-methyltetrahydrofuran-2-ylmethoxy]phenoxyphosphorylamino}propionic Acid 4-Fluorobenzyl Ester (23). Yield: 27.6%. ^{1}HNMR (DMSO-d_6): δ 1.20−1.27 (m, 6H), 3.80−3.98 (m, 2H), 4.01 (s, 1H), 4.25−4.26 (m, 1H), 4.37−4.38 (m, 1H), 5.07 (s, 2H), 5.52−5.56 (m, 1H), 5.86−5.87 (m, 1H), 5.99−6.05 (m, 1H), 6.15−6.17 (m, 1H), 7.15−7.21 (m, 5H), 7.36 (dd, J = 20.0, 8.0 Hz, 4H), 7.54 (s, 1H), 11.55 (s, 1H); MS, *m/e* 595.95 $(M + 1)^+$. HRMS, calcd for $C_{26}H_{29}F_2N_3O_9P$ $(M^+ + H)$, 596.1604; found, 596.1594.

(*S*)-2-[[(2*R*,3*R*,4*R*,5*R*)-5-(2,4-Dioxo-3,4-dihydro-2*H*-pyrimidin-1-yl)-4-fluoro-3-hydroxy-4-methyltetrahydrofuran-2-ylmethoxy]-(4-fluorophenoxy)phosphorylamino]propionic Acid Methyl Ester (24). Yield: 5.8%. ^{1}H NMR (DMSO-d_6) δ 1.28−1.34 (m, 6H), 3.65 (d, J = 4 Hz, 3H), 3.85−3.96 (m, 2H), 4.06−4.12 (m, 1H), 4.30−4.34 (m, 1H), 4.40−4.47 (m, 1H), 5.62−5.67 (m, 1H), 5.94−6.01 (m, 1H), 6.09 (d, J = 18.8 Hz, 1H), 6.17−6.26 (m, 1H), 7.27−7.33 (m, 4H), 7.62 (d, J = 7.6 Hz, 1H), 11.61 (s, 1H); MS, *m/e* 519.94 $(M + 1)^+$. HRMS, calcd for $C_{20}H_{25}F_2N_3O_9P$ $(M^+ + H)$, 520.1291; found, 520.1276.

(*S*)-2-{(4-Chlorophenoxy)-[(2*R*,3*R*,4*R*,5*R*)-5-(2,4-dioxo-3,4-dihydro-2*H*-pyrimidin-1-yl)-4-fluoro-3-hydroxy-4-methyltetrahydrofuran-2-ylmethoxy]phosphorylamino}propionic Acid Methyl Ester (25). Yield: 4.4%. ^{1}H NMR (DMSO-d_6) δ 1.23−1.28 (m, 6H), 3.58 (d, 2H), 3.81−3.89 (m, 2H), 3.99−4.02 (m,1H), 4.24−4.39 (m, 2H), 5.56−5.61 (t, 1H), 5.86−6.10 (m, 2H), 6.17−6.20 (m, 1H), 7.21−7.26 (m, 2H), 7.43−7.46 (m, 2H), 7.54−7.57 (d, 1H), 11.50 (s.1H); MS, *m/e* 536.1 $(M + 1)^+$. HRMS, calcd for $C_{20}H_{25}ClFN_3O_9P$ $(M^+ + H)$, 536.0995; found, 536.0981.

(*S*)-2-{(4-Bromophenoxy)-[(2*R*,3*R*,4*R*,5*R*)-5-(2,4-dioxo-3,4-dihydro-2*H*-pyrimidin-1-yl)-4-fluoro-3-hydroxy-4-methyltetrahydrofuran-2-ylmethoxy]phosphorylamino}propionic Acid Methyl Ester (26). Yield: 12%. ^{1}H NMR (DMSO-d_6) δ 1.20−1.26 (m, 6H), 3.57 (d, J = 2.8 Hz, 3H), 3.84 (s, 1H), 3.97−4.03 (m, 1H), 4.21−4.25 (m, 1H), 4.33−4.37 (m, 2H), 5.54−5.60 (m, 1H), 5.83−5.89 (m, 1H), 5.98−6.19 (m, 1H), 7.16 (t, J = 10.2 Hz, 2H), 7.52−7.57 (m, 3H), 11.52 (s, 1 H); MS, *m/e* 580 $(M + 1)^+$. HRMS, calcd for $C_{20}H_{25}BrFN_3O_9P$ $(M^+ + H)$, 580.0490; found, 580.0490.

(*S*)-2-{(3,4-Dichlorophenoxy)-[(2*R*,3*R*,4*R*,5*R*)-5-(2,4-dioxo-3,4-dihydro-2*H*-pyrimidin-1-yl)-4-fluoro-3-hydroxy-4-methyltetrahydrofuran-2-ylmethoxy]phosphorylamino}propionic Acid Methyl Ester (27). Yield: 4%. ^{1}H NMR (DMSO-d_6) δ 1.13 (m, 6H), 3.49 (s, 3H), 3.61−3.85 (m, 2H), 3.90−3.93 (m, 1H), 4.16−4.22 (m, 1H), 4.27−4.31 (m, 1H), 5.47−5.52 (m, 1H), 5.82 (d, J = 11.6 Hz, 1H), 5.93 (d, J = 19.2 Hz, 1H), 6.15−6.25 (m, 1H), 7.13 (t, J = 9.6 Hz, 1H), 7.43 (d, J = 12 Hz, 2H), 7.57 (d, J = 6.0 Hz, 1H), 11.43 (s, 1H); MS, *m/e* 569.85 $(M + 1)^+$. HRMS, calcd for $C_{20}H_{24}Cl_2FN_3O_9P$ $(M^+ + H)$, 570.0606; found, 570.0595.

(*S*)-2-{(2,4-Dichlorophenoxy)-[(2*R*,3*R*,4*R*,5*R*)-5-(2,4-dioxo-3,4-dihydro-2*H*-pyrimidin-1-yl)-4-fluoro-3-hydroxy-4-methyltetrahydrofuran-2-ylmethoxy]phosphorylamino}propionic Acid Methyl Ester (28). Yield: 11.5%. ^{1}H NMR (DMSO-d_6) δ 1.22−1.28 (m, 6H), 3.58−3.60 (m, 3H), 3.85−3.92 (m, 2H), 4.00−4.04 (m, 1H), 4.31−4.44 (m, 2 H), 5.55−5.61 (m, 1H), 5.86−6.10 (m, 2H), 6.33−6.39 (m, 1H), 7.44−7.54 (m, 3H), 7.72−7.75 (m, 1H), 11.54 (s.1H); MS, *m/e* 570.2 $(M + 1)^+$. HRMS, calcd for $C_{20}H_{24}Cl_2FN_3O_9P$ $(M^+ + H)$, 570.0606; found, 570.0597.

(*S*)-2-[[(2*R*,3*R*,4*R*,5*R*)-5-(2,4-Dioxo-3,4-dihydro-2*H*-pyrimidin-1-yl)-4-fluoro-3-hydroxy-4-methyltetrahydrofuran-2-ylmethoxy]-(naphthalen-1-yloxy)phosphorylamino]propionic Acid Methyl Ester (29). Yield: 18.3%. ^{1}H NMR (DMSO-d_6) δ 1.16−1.27 (m, 6H), 3.51−3.55 (d, 3H), 3.85−3.96 (m, 2H), 4.06−4.09 (m, 1H), 4.31−4.46 (m, 2H), 5.31−5.39 (m, 1H), 5.90−6.04 (m, 2H), 6.22−6.34 (m, 1H), 7.45−7.59 (m, 5H), 7.73−7.77 (m, 1H), 7.94−7.96 (m, 1H), 8.12−8.14 (m, 1H), 11.50 (s.1H); MS, *m/e* 552.1 $(M + 1)^+$. HRMS, calcd for $C_{24}H_{28}FN_3O_9P$ $(M^+ + H)$, 552.1542; found, 552.1529.

(*S*)-2-{[(2*R*,3*R*,4*R*,5*R*)-5-(2,4-Dioxo-3,4-dihydro-2*H*-pyrimidin-1-yl)-4-fluoro-3-hydroxy-4-methyltetrahydrofuran-2-ylmethoxy]ethoxyphosphorylamino}propionic Acid Methyl Ester (30). Yield: 43.8%. ^{1}H NMR (DMSO-d_6) δ 1.18−1.27 (m, 9H), 3.62 (s, 3H), 3.64−3.85 (m, 2H), 3.90−4.10 (m, 4H), 4.19−4.23 (m, 1H), 5.60−5.67 (m, 2H), 5.82−6.10 (m, 2H), 7.58−7.63 (m, 1H), 11.52 (s, 1H); MS, *m/e* 454.05 $(M + 1)^+$. HRMS, calcd for $C_{16}H_{26}FN_3O_9P$ $(M^+ + H)$, 454.1385; found, 454.1366.

{[(2*R*,3*R*,4*R*,5*R*)-5-(2,4-Dioxo-3,4-dihydro-2*H*-pyrimidin-1-yl)-4-fluoro-3-hydroxy-4-methyltetrahydrofuran-2-ylmethoxy]-phenoxyphosphorylamino}acetic Acid Methyl Ester (31). Yield: 22%. ^{1}H NMR (DMSO-d_6) δ 1.19−1.28 (m, 3H), 3.59 (s, 3H), 3.63−3.70 (m, 2H), 3.74−3.80 (m, 1H), 4.02 (d, J = 11.2 Hz, 1H), 4.23−4.28 (m, 1H), 4.40−4.43 (m, 1H), 5.57−5.59 (m, 1H), 5.89 (d, J = 6.8 Hz, 1H), 6.01−6.05 (m, 2H), 7.16−7.23 (m, 3H), 7.35−7.39 (m, 2H), 7.52(d, J = 8 Hz, 1H), 11.52 (s, 1H); MS, *m/e* 487.97 $(M + 1)^+$. HRMS, calcd for $C_{19}H_{24}FN_3O_9P$ $(M^+ + H)$, 488.1229; found, 488.1215.

(*S*)-2-{[(2*R*,3*R*,4*R*,5*R*)-5-(2,4-Dioxo-3,4-dihydro-2*H*-pyrimidin-1-yl)-4-fluoro-3-hydroxy-4-methyltetrahydrofuran-2-ylmethoxy]phenoxyphosphorylamino}butyric Acid Methyl Ester (32). Yield: 14%. ^{1}H NMR (DMSO-d_6) δ 0.72−0.79 (m, 3H), 1.18−1.25 (m, 3H), 1.42−1.61 (m, 2H), 3.53−3.57 (m, 3H), 3.58−3.80 (m, 2H), 3.91−4.02 (m, 1H), 4.12−4.38 (m, 2H),

5.54−5.59 (m,1H), 5.90−6.03 (m, 1H), 7.14−7.18 (m, 3H), 7.33−7.37 (m, 2H), 7.49 (t,1H), 11.45 (s, 1H); MS, *m*/*e* 515.95 $(M + 1)^+$; 1052.82 $(2M + 23)^+$. HRMS, calcd for $C_{21}H_{28}FN_3O_9P$ ($M^+ + H$), 516.1542; found, 516.1526.

(*S*)-2-{[(2*R*,3*R*,4*R*,5*R*)-5-(2,4-Dioxo-3,4-dihydro-2*H*-pyrimidin-1-yl)-4-fluoro-3-hydroxy-4-methyltetrahydrofuran-2-ylmethoxy]-phenoxyphosphorylamino}-3-methylbutyric Acid Methyl Ester (33). Yield: 20%. ^{1}H NMR (DMSO-d_6) δ 0.75−0.85 (m, 6H), 1.21−1.29 (m, 3H), 1.89−1.94 (m, 1H), 3.51−3.55 (m, 1H), 3.58 (d, J = 10.4 Hz, 3H), 3.72−3.95 (m, 1H), 4.03−4.05 (m, 1H), 4.23−4.37 (m, 2H), 5.56 (t, J = 16.0 Hz, 1H), 5.85−5.92 (m, 1H), 6.01−6.07 (m, 1H), 7.16−7.21 (m, 3H), 7.37 (t, J = 8 Hz, 2H), 7.55−7.60 (m, 1H), 11.52 (s, 1H); MS, *m*/*e* 530 $(M + 1)^+$. HRMS, calcd for $C_{22}H_{30}FN_3O_9P$ ($M^+ + H$), 530.1698; found, 530.1684.

(*S*)-2-{[(2*R*,3*R*,4*R*,5*R*)-5-(2,4-Dioxo-3,4-dihydro-2*H*-pyrimidin-1-yl)-4-fluoro-3-hydroxy-4-methyltetrahydrofuran-2-ylmethoxy]phenoxyphosphorylamino}-4-methylpentanoic Acid Methyl Ester (34). Yield: 21%. ^{1}H NMR (DMSO-d_6) δ 0.68−0.89 (m, 6H), 1.26 (d, J = 7.2 Hz, 3H), 1.41−1.64 (m, 3H), 3.70 (s, 3H), 3.73−3.79 (m, 2H), 3.99−4.04 (m, 1H), 4.19−4.27 (m, 1H), 4.34−4.38 (m, 1H), 5.55 (t, J = 9.0 Hz, 1H), 5.86−5.92 (m, 1H), 5.99−6.12 (m, 2H), 7.15−7.20 (m, 3H), 7.34−7.39 (m, 2H), 7.55 (s, 1H), 11.53 (s, 1H); MS, *m*/*e* 543.99 $(M + 1)^+$. HRMS, calcd for $C_{23}H_{32}FN_3O_9P$ ($M^+ + H$), 544.1855; found, 544.1841.

(*S*)-2-{[(2*R*,3*R*,4*R*,5*R*)-5-(2,4-Dioxo-3,4-dihydro-2*H*-pyrimidin-1-yl)-4-fluoro-3-hydroxy-4-methyltetrahydrofuran-2-ylmethoxy]phenoxyphosphorylamino}-4-methylsulfanylbutyric Acid Methyl Ester (35). Yield: 27.4%. ^{1}HNMR (DMSO-d_6): δ 1.25 (dd, J = 22.8 Hz, 5.6 Hz, 3H), 1.77−1.85 (m, 2H), 1.95 (d, J = 10.0 Hz, 3H), 2.31−2.36 (m, 1H), 2.40−2.44 (m, 1H), 3.59−3.64 (m, 3H), 3.88−3.91 (m, 2H), 4.05 (m, 1H), 4.25−4.26 (m, 1H), 4.29−4.40 (m, 1H), 5.56 (t, J = 8.0 Hz, 1H), 5.90−5.92 (m, 1H), 6.13−6.16 (m, 2H), 7.16−7.23 (m, 3H), 7.36−7.40 (m, 2H), 7.55 (d, J = 8.4 Hz, 1H), 11.51 (s, 1H); MS, *m*/*e* 562.52$(M + 1)^+$. HRMS, calcd for $C_{22}H_{30}FN_3O_9PS$ ($M^+ + H$), 562.1419; found, 562.1406.

(*S*)-2-{[(2*R*,3*R*,4*R*,5*R*)-5-(2,4-Dioxo-3,4-dihydro-2*H*-pyrimidin-1-yl)-4-fluoro-3-hydroxy-4-methyltetrahydrofuran-2-ylmethoxy]phenoxyphosphorylamino}-3-phenylpropionic Acid Methyl Ester (36). Yield: 6.6%. ^{1}H NMR (DMSO-d_6) δ 1.19−1.34 (m, 3H), 2.79−2.97 (m, 2H), 3.51−3.57 (m, 3H), 3.60−3.85 (m, 1H), 3.91−4.13 (m, 4H), 5.50−5.52 (m, 1H), 5.80−6.10 (m, 2H), 6.20−6.35 (m, 1H), 7.01−7.05 (m, 2H), 7.14−7.32 (m, 8H), 7.47 (s, 1H), 11.50 (s.1H); MS, *m*/*e* 578.2 $(M + 1)^+$. HRMS, calcd for $C_{26}H_{30}FN_3O_9P$ ($M^+ + H$), 578.1698; found, 578.1687.

(*S*)-2-{[(2*R*,3*R*,4*R*,5*R*)-5-(2,4-Dioxo-3,4-dihydro-2*H*-pyrimidin-1-yl)-4-fluoro-3-hydroxy-4-methyltetrahydrofuran-2-ylmethoxy]phenoxyphosphorylamino}-3-(1*H*-indol-3-yl)propionic Acid Methyl Ester (37). Yield: 8.1%. ^{1}H NMR (DMSO-d_6) δ 0.96 (d, J = 22.8 Hz, 3H), 2.90−2.94 (m, 1H), 3.03−3.08 (m, 1H), 3.42−3.48 (m, 3H) 3.60−3.65 (m, 1H), 3.92−3.94 (m, 2H), 4.17−4.19 (m, 2H), 5.48 (d, J = 8.4 Hz, 1H), 5.87 (d, J = 6.4 Hz, 1H), 5.95−6.00 (m, 1H), 6.21 (t, J = 11.4 Hz, 1H), 6.87−6.91 (m, 1H), 6.99−7.03 (m, 4H), 7.07−7.11 (m, 1H), 7.22−7.30 (m, 3H), 7.37 (d, J = 8 Hz 1H), 7.45 (d, J = 8 Hz, 1H), 10.80 (s, 1H), 11.48 (s, 1H); MS, *m*/*e* 616.96 $(M + 1)^+$; 1254.84 $(2M + 23)^+$. HRMS, calcd for $C_{28}H_{31}FN_4O_9P$ ($M^+ + H$), 617.1807; found, 617.1799.

2-[(*S*)-[(2*R*,3*R*,4*R*,5*R*)-5-(2,4-Dioxo-3,4-dihydro-2*H*-pyrimidin-1-yl)-4-fluoro-3-hydroxy-4-methyltetrahydrofuran-2-ylmethoxy]-(4-fluorophenoxy)phosphorylamino]-2-methylpropionic Acid Methyl Ester (38). Yield: 22%. ^{1}H NMR (DMSO-d_6) δ 1.19−1.36 (m, 9H), 3.54 (s, 3H), 3.56−3.89 (m, 1H), 4.00 (s, 1H), 4.22−4.26 (m, 1H), 4.35−4.38 (m, 1H), 5.52−5.55 (m, 1H), 5.87−6.04 (m, 3H), 7.17−7.23 (m, 4H), 7.58−7.60 (m, 1H), 11.55 (s, 1H); MS, *m*/*e* 534.01 $(M + 1)^+$. HRMS, calcd for $C_{21}H_{27}F_2N_3O_9P$ ($M^+ + H$), 534.1447; found, 534.1435.

1-[(*S*)-[(2*R*,3*R*,4*R*,5*R*)-5-(2,4-Dioxo-3,4-dihydro-2*H*-pyrimidin-1-yl)-4-fluoro-3-hydroxy-4-methyltetrahydrofuran-2-ylmethoxy]-(4-fluorophenoxy)phosphorylamino]cyclopropanecarboxylic Acid Methyl Ester (39). Yield: 40%. ^{1}H NMR (DMSO-d_6) δ 0.97−0.99 (m, 1H), 1.06−1.12 (m, 1H), 1.21−1.29 (m, 5H), 3.55 (s, 3H), 3.73−3.90 (m, 1H), 4.01 (s, 1H), 4.25−4.29 (m, 1H), 4.38−4.43 (m, 1H), 5.56−5.60 (m, 1H), 5.88 (s, 1H), 5.92−6.10 (m, 1H), 6.59 (t, J = 16 Hz, 1H), 7.21−7.23 (m, 4H), 7.56 (dd, J = 8.0, 28.0 Hz, 1H), 11.55 (s, 1H); MS, *m*/*e* 532.00 $(M + 1)^+$. HRMS, calcd for $C_{21}H_{25}F_2N_3O_9P$ ($M^+ + H$), 532.1291; found, 532.1280.

(*R*)-2-{[(2*R*,3*R*,4*R*,5*R*)-5-(2,4-Dioxo-3,4-dihydro-2*H*-pyrimidin-1-yl)-4-fluoro-3-hydroxy-4-methyltetrahydrofuran-2-ylmethoxy]phenoxyphosphorylamino}propionic Acid Isopropyl Ester (40). Yield: 8.57%. ^{1}H NMR (DMSO-d_6) δ 1.19−1.29 (m, 12H), 3.65−3.75 (m, 2H), 3.95−4.05 (m, 1H), 4.24−4.25 (m, 1H), 4.35−4.37 (m, 1H), 4.84−4.86 (m, 1H), 5.53−5.61 (m, 1H), 5.88 (m, 1H), 6.01−6.14 (m, 2H), 7.14−7.39 (m, 5H), 7.48−7.60 (m, 1H), 11.53 (s, 1H); MS, *m*/*e* 529.96 $(M + 1)^+$. HRMS, calcd for $C_{22}H_{30}FN_3O_9P$ ($M^+ + H$), 530.1698; found, 530.1684.

(*S*)-2-[[(2*R*,3*R*,4*R*,5*R*)-5-(2,4-Dioxo-3,4-dihydro-2*H*-pyrimidin-1-yl)-4-fluoro-3-hydroxy-4-methyltetrahydrofuran-2-ylmethoxy]-(4-fluorophenoxy)phosphorylamino]propionic Acid Ethyl Ester (41). Yield: 15.4%. ^{1}H NMR (DMSO-d_6) δ 1.13−1.28 (m, 9H), 3.72−3.94(m, 2H), 3.98−4.10 (m, 3H), 4.21−4.42 (m, 2H), 5.56−5.61 (m, 1H), 5.85−6.20 (m, 3H), 7.21−7.24 (m, 4H), 7.55−7.58 (d, 1H), 11.50 (s, 1H); ^{13}C NMR (DMSO-d_6) δ 174.01, 173.97, 173.87, 163.60, 160.87, 158.48, 151.32, 147.65, 140.34, 130.52, 122.73, 122.68, 122.65, 120.92, 117.14, 116.90, 103.21, 102.10, 100.29, 89.53, 80.32, 72.40, 72.22, 65.41, 61.46, 61.43, 50.72, 50.60, 20.70, 20.63, 20.56, 20.49, 17.53, 17.28, 14.82; MS, *m*/*e* 533.90 $(M + 1)^+$; HRMS, calcd for $C_{21}H_{27}F_2N_3O_9P$ ($M^+ + H$), 534.1453; found, 534.1434.

(*S*)-2-{(4-Chlorophenoxy)-[(2*R*,3*R*,4*R*,5*R*)-5-(2,4-dioxo-3,4-dihydro-2*H*-pyrimidin-1-yl)-4-fluoro-3-hydroxy-4-methyltetrahydrofuran-2-ylmethoxy]phosphorylamino}propionic Acid Ethyl Ester (42). Yield: 30.17%. ^{1}H NMR (DMSO-d_6) δ 1.14 (t, J = 7.0 Hz, 3H), 1.21−1.28 (m, 6H),3.77−3.89 (m, 2H), 4.00−4.08 (m, 3H), 4.24−4.27 (m, 1H), 4.34−4.43 (m, 1H), 5.56−5.61 (m, 1H), 5.86−6.13 (m, 2H), 6.17−6.24 (m, 1H), 7.21−7.26 (m, 2H), 7.44 (d, J = 7.6 Hz, 2H), 7.55 (d, J = 7.6 Hz, 1H), 11.55 (s, 1H); MS, *m*/*e* 549.11 $(M + 1)^+$; HRMS, calcd for $C_{21}H_{27}ClFN_3O_9P$ ($M^+ + H$), 550.1157; found, 550.1141.

(*S*)-2-{(4-Bromophenoxy)-[(2*R*,3*R*,4*R*,5*R*)-5-(2,4-dioxo-3,4-dihydro-2*H*-pyrimidin-1-yl)-4-fluoro-3-hydroxy-4-methyltetrahydrofuran-2-ylmethoxy]phosphorylamino}propionic Acid Ethyl Ester (43). Yield: 35.86%. ^{1}H NMR (DMSO-d_6) δ 1.13 (t, J = 7.2 Hz, 3H), 1.16−1.28 (m, 6H), 3.78−3.86 (m, 2H), 4.01−4.07 (m, 3H), 4.24−4.28 (m, 1H), 4.39−4.40 (m, 1H), 5.56−5.61 (m, 1H), 5.82−5.90 (m, 1H), 5.93−6.07 (m, 1H), 6.14−6.19 (m, 1H), 7.18 (dd, J = 11.2, 8.8 Hz, 2H), 7.53−7.58 (m, 3H), 11.53 (s, 1H); MS, *m*/*e* 593.90$(M + 1)^+$. HRMS, calcd for $C_{21}H_{27}BrFN_3O_9P$ ($M^+ + H$), 594.0652; found, 594.0640.

(*S*)-2-[[(2*R*,3*R*,4*R*,5*R*)-5-(2,4-Dioxo-3,4-dihydro-2*H*-pyrimidin-1-yl)-4-fluoro-3-hydroxy-4-methyltetrahydrofuran-2-ylmethoxy]-(4-fluorophenoxy)phosphorylamino]propionic Acid Isopropyl Ester (44). Yield: 11.3%. ^{1}H NMR (DMSO-d_6) δ 1.14−1.28 (m, 12H), 3.74−3.84 (m,2H), 3.99−4.06 (m, 1H), 4.23−4.39 (m, 2H), 4.83−4.86 (m, 1H), 5.56−5.60 (t, 1H), 5.85−6.12 (m, 3H), 7.19−7.24 (m, 4H), 7.56−7.57 (d, 1H), 11.50 (s, 1H); MS, *m*/*e* 547.91 $(M + 1)^+$. HRMS, calcd for $C_{22}H_{29}F_2N_3O_9P$ ($M^+ + H$), 548.1604; found, 548.1591.

(*S*)-2-{(4-Chlorophenoxy)-[(2*R*,3*R*,4*R*,5*R*)-5-(2,4-dioxo-3,4-dihydro-2*H*-pyrimidin-1-yl)-4-fluoro-3-hydroxy-4-methyltetrahydrofuran-2-ylmethoxy]phosphorylamino}propionic Acid Isopropyl Ester (45). Yield: 24%. ^{1}H NMR (DMSO-d_6) δ 1.05−1.19 (m, 12H), 3.76−3.80 (m, 2H), 3.98−4.08 (m, 1H), 4.31 (m, 2H), 4.73−4.77 (m, 1H), 5.49−5.54 (m, 1H), 5.80−6.20 (m, 3H), 7.20−7.2 5 (m, 2H), 7.43 (d, J = 8.8 Hz, 1H), 7.54 (d, J = 8 Hz, 1H), 11.51

(s, 1H); ^{13}C NMR (DMSO-d_6) δ 173.63, 173.59, 173.54, 173.48, 163.71, 151.39, 150.47, 150.42, 140.30, 130.51, 129.61, 122.95, 122.90, 122.83, 103.31, 103.23, 102.18, 100.39, 89.43, 80.32, 72.37, 69.04, 68.99, 65.85, 65.43, 50.86, 50.71, 22.35, 22.34, 22.31, 20.78, 20.71, 20.64, 20.57, 17.62, 17.37; MS, *m*/*e* 563.88 $(M + 1)^+$; 1148.73 $(2M + 23)^+$. HRMS, calcd for $C_{22}H_{29}ClFN_3O_9P$ ($M^+ + H$), 564.1308; found, 564.1297.

(*S*)-2-{(4-Bromophenoxy)-[(2*R*,3*R*,4*R*,5*R*)-5-(2,4-dioxo-3,4-dihydro-2*H*-pyrimidin-1-yl)-4-fluoro-3-hydroxy-4-methyltetrahydrofuran-2-ylmethoxy]phosphorylamino}propionic Acid Isopropyl Ester (46). Yield: 21.2%. ^{1}H NMR (DMSO-d_6): δ 1.10−1.14 (m, 6H), 1.20−1.28 (m, 6H), 3.77−3.82 (m, 2H), 3.99−4.01 (m, 1H), 4.21−4.25 (m, 1H), 4.37−4.38 (m, 1H), 4.81−4.86 (m, 1H), 5.58 (dd, J = 8.0, 4.0 Hz, 1H), 5.82−5.95 (m, 1H), 5.96−6.09 (m, 1H), 6.10−6.14 (m, 1H), 7.18 (dd, J = 12.0, 8.0 Hz, 2H), 7.54−7.57 (m, 3H), 11.52 (s, 1H); MS, *m*/*e* 607.90 $(M + 1)^+$; 1238.64 $(2M + 23)^+$. HRMS, calcd for $C_{22}H_{29}BrFN_3O_9P$ ($M^+ + H$), 608.0803; found, 608.0795.

(*S*)-2-[[(2*R*,3*R*,4*R*,5*R*)-5-(2,4-Dioxo-3,4-dihydro-2*H*-pyrimidin-1-yl)-4-fluoro-3-hydroxy-4-methyltetrahydrofuran-2-ylmethoxy]-(4-fluorophenoxy)phosphorylamino]propionic Acid Cyclohexyl Ester (47). Yield: 9.5%. ^{1}H NMR (DMSO-d_6) δ 1.20−1.44 (m, 12H), 1.62−1.71 (m, 4H), 3.75−4.02 (m, 2H), 3.94−4.02 (m, 1H), 4.19−4.26 (m, 2H), 4.59−4.61 (m, 1H), 5.57 (t, J = 8.4 Hz, 1H), 5.85−6.06 (m, 3H), 7.17−7.23 (m, 4H), 7.54 (d, J = 8.4 Hz, 1H), 11.51 (s, 1H); ^{13}C NMR (DMSO-d_6) δ 173.58, 173.54, 163.70, 160.94, 158.55, 151.40, 147.76, 140.20, 122.85, 122.81, 122.76, 122.72, 122.68, 117.25, 117.02, 103.30, 102.18, 100.39, 89.40, 80.32, 73.53, 73.48, 72.38, 65.86, 65.36, 50.90, 50.74, 31.79, 31.72, 25.75, 23.94, 20.88, 20.81, 20.74, 20.68, 17.60, 17.35; MS, *m*/*e* 587.92 $(M + 1)^+$. HRMS, calcd for $C_{25}H_{33}F_2N_3O_9P$ ($M^+ + H$), 588.1917; found, 588.1906.

(*S*)-2-{(4-Chlorophenoxy)-[(2*R*,3*R*,4*R*,5*R*)-5-(2,4-dioxo-3,4-dihydro-2*H*-pyrimidin-1-yl)-4-fluoro-3-hydroxy-4-methyltetrahydrofuran-2-ylmethoxy]phosphorylamino}propionic Acid Cyclohexyl Ester (48). Yield: 13.7%. ^{1}HNMR (DMSO-d_6): δ 1.21−1.46 (m, 12H), 1.62−1.69 (m, 4H), 3.77−3.83 (m, 2H), 3.98−4.10 (m, 1H), 4.26 (s, 1H), 4.32−4.45 (m, 1H), 4.61 (s, 1H), 5.55−5.60 (m, 1H), 5.82−5.95 (m, 1H), 5.98−6.20 (m, 2H), 7.21−7.26 (m, 2H), 7.43 (d, J = 8.8 Hz, 2H), 7.54 (d, J = 8.0 Hz, 1H), 11.55 (s, 1H); MS, *m*/*e* 603.97 $(M + 1)^+$, 626.10 $(M + 23)^+$. HRMS, calcd for $C_{25}H_{33}ClFN_3O_9P$ ($M^+ + H$), 604.1621; found, 604.1615.

(*S*)-2-{(4-Bromophenoxy)-[(2*R*,3*R*,4*R*,5*R*)-5-(2,4-dioxo-3,4-dihydro-2*H*-pyrimidin-1-yl)-4-fluoro-3-hydroxy-4-methyltetrahydrofuran-2-ylmethoxy]phosphorylamino}propionic Acid Cyclohexyl Ester (49). Yield: 13.7%. ^{1}HNMR (DMSO-d_6): δ 1.19−1.46 (m, 12H), 1.62−1.69 (m, 4H), 3.76−3.83 (m, 2H), 3.95−4.08 (m, 1H), 4.25−4.28 (m, 1H), 4.38 (s, 1H), 4.60−4.62 (m, 1H), 5.56−5.61 (m, 1H), 5.82−5.95 (m, 1H), 6.02−6.20 (m, 2H), 7.09−7.20 (m, 2H), 7.53−7.57 (m, 3H), 11.53 (s, 1H); MS, *m*/*e* 650.0 $(M + 3)^+$. HRMS, calcd for $C_{25}H_{33}BrFN_3O_9P$ ($M^+ + H$), 648.1116; found, 648.1114.

Crystallization of 50 from Column Purified Amorphous 50. The chromatographed fraction containing the first eluting isomer (**50**, 3.8 g, 97% pure) was dissolved in isopropanol (36 g) and diluted with heptanes until cloudy (72 g). The solution was seeded and stirred at ambient temperature for 5 h. The resulting solid was collected by vacuum filtration, washed with heptanes (2 × 20 mL), and dried (50 °C, 0.2 mm, 24 h) to 2.3 g of very small white needles that were not suitable for single crystal X-ray analysis: mp 136.2−137.8 °C; HPLC purity, 99.02%.

Crystallization of 51 from Column Purified Mixture 14. An amount of 40.0 g of an approximately 1:1 mixture of **14** prepared in a similar manner was dissolved in dichloromethane (90 mL). Diisopropyl ether (70 mL) was added to the above solution to give a saturated solution. The solution was seeded with pure **51**, and the mixture was gently stirred with a stir bar at room temperature for 20 h.. The solid was filtered, washed with a mixture of diisopropyl ether/dichloromethane (40 mL, 1:1 v/v), and dried to give white solid (16.6 g, 89.35% pure **51** by ^{31}P NMR). This solid was suspended in dichloromethane (83 mL) and heated to reflux for 3 h. The suspension was cooled to ambient temperature and stirred overnight. The solid was filtered and washed with cold dichloromethane (10 mL). The solid was dried under vacuum to give **51** (13.1 g, 99.48% pure by HPLC). Then 11 g of this solid was redissolved in DCM (330 mL), and the mixture was heated to reflux. The solution was cooled to ambient temperature and left at this temperature overnight without stirring. The product was filtered and dried (25 °C, 0.2 mm, 24 h) to give 10.5 g of **51** (99.74% by HPLC) as large white needles in 53% recovered theoretical yield of the single isomer.

Crystallization of 51 from Crude Mixture of 14. To a stirred solution of L-alanine isopropyl ester hydrochloride (10.5 g, 61.5 mmol, azeotropically dried, two times, with 50 mL of toluene each time) in dichloromethane (100 mL) was added phenyl dichlorophosphate (7.5 mL, 50 mmol) at ambient temperature. The mixture was cooled to −10 °C, and then a solution of NMI (30.5 mL, 384 mmol) in 30 mL of dichloromethane was added over a period of 30 min. After completion of the addition, the mixture was stirred between −10 and −15 °C for 1 h. To the above mixture was added 2′-deoxy-2′-fluoro-2′-*C*-methyluridine (**5**, 10 g, 38.4 mmol) in one lot, and the mixture was stirred below −10 °C for 3 h and then slowly allowed to warm to 20 °C (6 h). The mixture was stirred at this temperature overnight (15 h) and then quenched with 10 mL of methanol. The solvent was evaporated, and the residue was redissolved in EtOAc (200 mL). The EtOAc layer was washed with water (100 mL), 1 N HCl (3 × 75 mL), 2% aqueous $NaHCO_3$ solution (50 mL), and brine (50 mL). The organic layer was dried over Na_2SO_4, filtered, and concentrated. The residue was dried under high vacuum for 2 h to give white foam (22 g). The above foam was dissolved in 33 mL of DCM, and then 65 mL of IPE (isopropyl ether) was added to give a saturated solution. The solution was filtered though a small pad of Celite, and the filtrate was stirred with **51** seeds for 72 h at ambient temperature. The white solid was filtered, washed with IPE (20 mL), and dried to give 4.58 g of a white powder which was determined by ^{31}P NMR to be an 85:15 mixture of **51**/**50**. The above solid was suspended in DCM (23 mL), and then the mixture was refluxed for 3 h. The mixture was cooled to room temperature and stirred for 15 h. The white solid was filtered, washed with cold DCM (4.5 mL), and dried under high vacuum at 45 °C to give 3.11 g of **51** (HPLC purity 99.74%, mp 93.9−104.7 °C) in 15.2% yield from **6**.

X-ray Structure Determination of Compound 51. Compound **51**, $C_{23}H_{31}N_3PO_9FCl_2$, crystallizes in the monoclinic space group $P2_1$ (systematic absences $0k0$, k = odd) with a = 12.8822(14) Å, b = 6.1690(7) Å, c = 17.733(2) Å, β = 92.045(3)°, V = 1408.4(3) Å^3, Z = 2, and d_{calc} = 1.449 g/cm^3. X-ray intensity data were collected on a Rigaku mercury CCD area detector employing graphite-monochromated Mo Kα radiation (λ = 0.710 73 Å) at 143 K. Preliminary indexing was performed from a series of 12 0.5° rotation images with exposures of 30 s. A total of 648 rotation images were collected with a crystal to detector distance of 35 mm, a 2θ swing angle of −12°, rotation widths of 0.5°, and exposures of 30 s: scan no. 1 was a ϕ-scan from 315° to 525° at ω = 10° and χ = 20°; scan no. 2 was an ω-scan from −20° to 5° at χ = −90° and ϕ = 315°; scan no. 3 was an ω-scan from −20° to 4° at χ = −90° and ϕ = 135°; scan no. 4 was an ω-scan from −20° to 5° at χ = −90° and ϕ = 225°; scan no. 5 was an ω-scan from −20° to 20° at χ = −90° and ϕ = 45°. Rotation images were processed using CrystalClear (Rigaku Corp., 1999), producing a listing of unaveraged F^2 and $\sigma(F^2)$ values which were then passed to the CrystalStructure (Crystal Structure Analysis Package, Rigaku Corp., 2002) program package for further processing and structure solution on a Dell Pentium III computer. A total of 7707 reflections were measured over the ranges 5.48° ≤ 2θ ≤ 50.04°, −14 ≤ h ≤ 15,

$-7 \le k \le 6$, $-19 \le l \le 21$, yielding 4253 unique reflections ($R_{int} = 0.0180$). The intensity data were corrected for Lorentz and polarization effects and for absorption using REQAB (minimum and maximum transmission of 0.824 and 1.000).

The structure was solved by direct methods (SIR97).[41] Refinement was by full-matrix least squares based on F^2 using SHELXL-97.[42] All reflections were used during refinement. The weighting scheme used was $w = 1/[\sigma^2(F_o^2) + 0.0472P^2 + 0.4960P]$ where $P = (F_o^2 + 2F_c^2)/3$. Non-hydrogen atoms were refined anisotropically, and hydrogen atoms were refined using a "riding" model. Refinement converged to R1 = 0.0328 and wR2 = 0.0817 for 4046 reflections for which $F > 4\sigma(F)$ and R1 = 0.0348, wR2 = 0.0838, and GOF = 1.056 for all 4253 unique, nonzero reflections and 358 variables. The maximum Δ/σ in the final cycle of least squares was 0.000, and the two most prominent peaks in the final difference Fourier were +0.312 and −0.389 e/Å^3. The Flack absolute structure parameter was refined to −0.06(6), thus corroborating the stereochemistry of the title compound.

Biological Assays. HCV Replicon Assay. HCV replicon assays using clone A cells and ET-lunet cells were performed as described previously .[13] Briefly, clone A cells and ET-lunet cells were seeded at a density of 1500 and 3000 cells per well in a 96-well plate, respectively. Test compounds serially diluted in culture medium without G418 were added to cells. Plates were incubated at 37 °C in a 5% CO_2 atmosphere for 4 days. Inhibition of HCV RNA replication was determined by quantitative real time PCR.[12]

To express the antiviral effectiveness of a compound, the threshold RT-PCR cycle of the test compound was subtracted from the average threshold RT-PCR cycle of the no-drug control (ΔCt_{HCV}). A ΔCt of 3.3 equals a 1 − log 10 reduction (equal to the 90% effective concentration [EC_{90}]) in replicon RNA levels. The cytotoxicity of the test compound could also be expressed by calculating the ΔCt_{rRNA} values. The $\Delta\Delta Ct$ specificity parameter could then be introduced ($\Delta Ct_{HCV} - \Delta Ct_{rRNA}$), in which the levels of HCV RNA are normalized for the rRNA levels and calibrated against the no-drug control.

Cell Cytotoxicity Assays. Each compound (serially diluted from 100 μM) was added to Huh7 (2×10^3 cells/well), HepG2 (2×10^3 cells/well), BxPC3 (2×10^3 cells/well), or CEM (5×10^3 cells/well) cells and allowed to incubate for 8 days at 37 °C. A medium only control was used to determine the minimum absorbance value and an untreated cell. At the end of the growth period, MTS dye from the CellTiter 96 AQueous One Solution Cell Proliferation Assay kit (Promega) was added to each well, and the plate was incubated for an additional 2 h. The absorbance at 490 nm was read with a Victor3 plate reader (Perkin-Elmer) using the medium only control wells as blanks. The 50% inhibition value (CC_{50}) was determined by comparing the absorbance in wells containing cells and test compound to untreated cell control wells.

Mitochrondria Toxicity Assay. Each compound or ddC was serially diluted from 100 μM in assay medium and was added to HepG2, BxPC3, or CEM cells seeded at 1×10^4 cells/well in a 24-well plate. Cells were incubated at 37 °C in a humidified 5% CO_2 atmosphere for 14 days. On days 7 and 11 medium was removed and replenished with fresh medium containing the appropriate concentration of compound. On day 14, cells were harvested and total cellular DNA was extracted as recommended by the manufacturer (Qiagen). The mitochondrial cytochrome C oxidase subunit II (COXII) gene and rDNA were amplified using a multiplex quantitative RT-PCR protocol. The ΔCt of mitochondrial COXII DNA (mtDNA) and ΔCt of rDNA (rDNA) for each sample were determined as described previously.[43] ΔCt was converted to log reduction of mtDNA or rDNA, and percent inhibition was determined relative to the untreated cell controls. Toxicity levels were expressed as the concentration inhibiting mtDNA and rDNA by 90%.

Human Bone Marrow Cytotoxicity Assay. The proliferation of human erythroid and myeloid hematopoietic progenitor cells derived from normal bone marrow (Lonza, Walkersville, MD) was assessed in a semisolid methylcellulose-based medium (R&D Systems, Minneapolis, MN) containing recombinant human (rh-) stem cell factor (50 ng/mL), rh-interleukin-3 (10 ng/mL), rh-granulocyte/monocyte-colony stimulating factor (10 ng/mL), and rh-erythropoietin (3 U/mL). Increasing concentrations of each compound (up to 50 μM) diluted in DMSO were added to progenitor cells seeded at 2×10^4 cells per culture in the methylcellulose-based medium. Each compound or the DMSO (0.1%) control were incubated with the progenitor cells for 14−16 days in culture, after which the proliferated colonies were assessed and scored based on size and morphology to determine 50% inhibition concentration as described previously.[35,36]

Simulated Gastric Fluid (SGF) and Simulated Intestinal Fluid (SIF) Stability Assay. Stock solutions of each compound (10 mg/mL) were prepared in DMSO and stored at −20 °C. An amount of 5 μL of the stock solution was added to 995 μL of simulated gastric fluid (SGF without pepsin, RICCA Chemical Co.) or simulated intestinal fluid (SIF without pancreatin, RICCA Chemical Co.) to give the working solution (50 μg/mL). The working solution was immediately analyzed by HPLC to obtain the initial ($T = 0$) absorbance value for the compound (peak area at 260 nm). The sample was repeatedly injected every 2 h over a 20 h time period with the autosampler set at 37 °C. Each compound was analyzed by reverse phase HPLC with an Eclipse XDB-C18 5 μm column (Agilent) using a Alliance system (Waters). The mobile phase consisted of solvent A (Water with 50 mM triethylammonium acetate) and solvent B (acetonitrile). Elution was performed using a linear gradient of solvent B from 20% to 98% for 5 min. The amount of parent compound was determined on the basis of the peak area at each time point, and the percentage remaining was calculated on the basis of the initial amount measured at 0 h.

Compound Stability in Human Liver S9 Fraction. Stock solutions of each compound (50 mM) were prepared in DMSO and stored at −20 °C. The reaction mixture was prepared in a total volume of 1 mL containing 5 mM of $MgCl_2$, 50 mM of K_2HPO_4 (pH 7.4), and 100 μM compound. The reaction was initiated by adding 4 mg/mL human liver S9 fraction (CellzDirect) to the reaction mixture and incubated at 37 °C. At the desired times (0, 0.5, 1, 2, 4, 6, 8, and 24 h), 100 μL aliquots were taken and the reaction was stopped by mixing the reaction mixture sample with 300 μL of acetonitrile. The samples were centrifuged at 14 000 rpm for 30 min at 4 °C. Then 100 μL of the supernatant was mixed with 100 μL of LC/MS solvent A (95% water, 5% acetonitrile, 10 mM ammonium acetate, and 0.01% formic acid) and frozen at −20 °C. The standard solutions of each compound was prepared from 10 mg/mL of stock solution and diluted to a final concentration of 1 μg/mL in methanol. The standard solutions were injected into the LC/MS to determine the daughter ion, cone voltage, and collision energy in order to develop the LC/MS/MS method. Each compound was separated by using a Phenomenex Luna 5 μm C18 column with a Waters Alliance system. The mobile phase consisted of solvent A (95% water, 5% acetonitrile, 10 mM ammonium acetate, and 0.01% formic acid) and solvent B (95% acetonitrile, 5% water, 10 mM ammonium acetate, and 0.01% formic acid). Elution was performed using a linear gradient of solvent B from 0% to 100% for 2.5 min. The MS/MS detection was performed by using Micromass Quattro Micro with cone voltage 35 and collision energy 20 eV. The samples collected at the desired time points were thawed, and 10 μL aliquots were used for LC/MS/MS analysis. The amount of parent compound was determined on the basis of the peak area for each time point, and the percentage remaining was calculated on the basis of the initial amount measured at 0 h. The half-life of each compound, which is a measure of the stability of the compound, was calculated by using the GraphPad Prism software.

Compound Stability in Human Plasma. Stock solutions of each compound were prepared in DMSO and stored at −20 °C. Then 1 mL of human plasma containing 5 mM $MgCl_2$ was used for the reaction. The reaction was started by adding 2 μL of a 50 mM stock solution of each compound to give a final concentration of 100 μM and incubated at 37 °C. At the desired times (0, 0.5, 1, 2, 4, 6, 8, and 24 h), 100 μL aliquots were taken and the reaction was stopped by mixing the reaction mixture sample with 200 μL of acetonitrile. The samples were centrifuged at 14 000 rpm for 30 min at 4 °C. Then 100 μL of the supernatant was mixed with 100 μL of LC/MS solvent A (95% water, 5% acetonitrile, 10 mM ammonium acetate, and 0.01% formic acid) and frozen at −20 °C. The standard solution of each compound was prepared from 10 mg/mL stock solution and diluted to a final concentration of 1 μg/mL in methanol. The standard solutions were injected into the LC/MS to determine the daughter ion, cone voltage, and collision energy in order to develop the LC/MS/MS method. Each compound was separated by using a Phenomenex Luna 5 μm C18 column (Phenomenex) with a Waters Alliance system (Waters). The mobile phase consisted of solvent A (95% water, 5% acetonitrile, 10 mM ammonium acetate, and 0.01% formic acid) and solvent B (95% acetonitrile, 5% water, 10 mM ammonium acetate, and 0.01% formic acid). Elution was performed using a linear gradient of solvent B from 0% to 100% for 2.5 min. The MS/MS detection was performed by using Micromass Quattro Micro (Waters) with cone voltage 35 and collision energy 20 eV. The samples collected at the desired time points were thawed, and 10 μL aliquots were used for LC/MS analysis. The amount of parent compound based on the peak area was determined for each time point and the percentage remaining was calculated on the basis of the initial amount measured at 0 h. The half-life of each compound was calculated by using the GraphPad Prism software.

Parallel Artificial Membrane Permeability Assay (PAMPA). A 96-well filtration plate (PVDF membrane, pore size 0.45 μm, Millipore, Billerica, MA) coated with 5 μL of lecithin in dodecane (20 mg/mL) was used as donor plate. The donor plate was filled with 200 μL of PBS buffer (pH 7.4, Gibco) containing 200 μg/mL test compound and 2% of DMSO. The acceptor plate was filled with 300 μL of PBS buffer with 2% of DMSO. The donor filter plate was carefully put on the acceptor plate to form a sandwich, which was left undisturbed for 24 h. The concentration of compounds in the donor and acceptor wells after incubation was determined by LC/MS/MS, which consisted of a Waters Alliance HT 2795 separations module, a Waters Quattro Micro API triple quadrupole mass spectrometer (Milford, MA), and a Ascentis phenylhexyl column (4.6 mm × 30 mm, 2.7 μm partical, Supelco, Bellefonte, PA). The mass spectrometer was operated in MRM mode for quantitation. The permeability is determined using the following equations: $P_e = [-\ln(1 - C_A/C_{eq})]/[A(1/V_D + 1/V_A)t]$, $C_{eq} = (C_D V_D + C_A V_A)/(V_D + V_A)$, where C_D is the compound concentration in donor well, C_A is the compound concentration in acceptor well, V_D is the donor well volume, V_A is the acceptor well volume, C_{eq} is the concentration at equilibrium, A is the filter area, and t is the incubation time.

In Vitro Determination of Triphosphate Levels in Primary Human, Rat, Dog, and Monkey Hepatocytes. Clone A cells and primary hepatocytes were seeded (5 000 000 cells) into T75 flasks in DMEM containing 10% FBS and primary cell plating medium (CellzDirect, Inc.), respectively. After overnight incubation to allow the cells to attach, the cells were incubated for up to 24 h at 37 °C in a 5% CO_2 atmosphere in the fresh medium containing 100 μM test compound. At selected times, extracellular medium was removed and the cell layer was washed with cold PBS. After trypsinization, cells were counted and centrifuged at 1200 rpm for 5 min. The cell pellets were resuspended in 1 mL of cold 60% methanol and incubated overnight at −20 °C. The samples were centrifuged at 14 000 rpm for 5 min, and the supernatants were collected and dried using a SpeedVac concentrator, then stored at −20 °C until they were to be analyzed by HPLC. Residues were suspended in 100 μL of water, and 50 μL aliquots were injected into the HPLC instrument. HPLC analysis was performed as previously described.[19]

Rat in Vivo Liver Triphosphate Analysis. Each compound was dosed orally by gavage with a single dose of compound at 50 mg/kg to rats in a volume of 5 mL/kg in 0.5% carboxymethylcellulose sodium. Liver samples were removed at time points 0.5, 1, 2, 4, 6, and 12 h postdose by first sacrificing the animal by CO_2 inhalation, perfusing the liver with ice cold saline and removing approximately 1 g of liver, which was then snap-frozen in liquid nitrogen and stored at −80 °C. Live samples were homogenized in 3 volumes of ice cold 70% methanol containing 20 mM EDTA/EGTA. Samples were centrifuged at 3000*g* for 15 min, and aliquots of the supernatant (100 μL) were evaporated to dryness. The resulting dried residue was reconstituted with 100 μL of mobile phase and analyzed for **6** by LC/MS/MS. LC conditions were as follows: Shiseido SI-2 3301 HPLC instrument; column, Agela venusil XBP C8 2.1 mm × 50 mm; 30 °C column temperature; mobile phase of (A) 0.1% formic acid in water, (B) 0.1% formic acid in acetonitrile; flow rate of 0.45 mL/min; gradient of 0−3 min; time, 0 min at 5% B and 95% A, 1.4 min at 100% A, 2 min at 5% A and 95% B, 3 min at 5% A and 95% B. Mass spectometer conditions were as follows: Thermo TSQ Quantum Ultra, electospray ionization, MRM negative mode, spray voltage 3500 V. Liver concentrations versus time data were analyzed by noncompartmental approaches using the WinNonlin software, version 5.0.1.

Dog and Cynomolgus Monkey in Vivo Pharmacokinetic Analysis. Compounds **12**, **14**, and **47** were each dosed orally by gavage (dog, gastric; monkey, nasogastric) at a dose of 50 mg/kg in hydroxypropyl-β-cyclodextrin in water (20% w/v) for 4 consecutive days. Dose volume was 2.5 mL/kg. Serial blood samples were collected at 1, 2, 4, 6, 12, and 24 postdose after dose administration on day 3. All blood samples were obtained by venipuncture into polypropylene tubes containing K_2EDTA (10 mL, 0.5 M) and kept on ice for processing by centrifugation. Plasma samples were quick-frozen over dry ice and kept at −70 °C until LC/MS/MS analysis. At the 4 h time point postdose on day 4, the animals were anesthetized using pentobarbital. Ice cold saline was perfused into the liver via a portal cannula. Five samples from various liver lobes (10 g each) were harvested, weighed, and snap-frozen in liquid nitrogen. Frozen liver samples were homogenized in three volumes of ice cold 70% methanol containing 20 mM EDTA/EGTA. The amount of compound **6** was quantified by LC/MS/MS. LC conditions were as follows: Shiseido SI-2 3301 HPLC instrument; column, Agela venusil XBP C8 2.1 mm × 50 mm; 30 °C column temperature; mobile phase of (A) 0.1% formic acid in water, (B) 0.1% formic acid in acetonitrile; flow rate of 0.45 mL/min; gradient of 0−3 min; time, 0 min at 5% B and 95%A, 1.4 min at 100% A, 2 min at 5% A and 95% B, 3 min at 5% A and 95% B. Mass spectometer conditions were as follows: Thermo TSQ Quantum Ultra, electospray ionization, MRM negative mode, spray voltage 3500 V. Plasma and liver concentrations versus time data were analyzed by noncompartmental approaches using the WinNonlin software program, version 5.0.1.

Single Dose in Vivo Rat Toxicology Assessment. For each compound, 24 (12 per sex) rats (*Rattus norvegicus*; breed, CDIGS-Crl:CD(SD); source, Charles River Laboratories, Wilmington, MA; age, 4−5 weeks; body weight, 76−100 g) were dosed with compound or vehicle (30% PEG400/30% Tween 20/20% corn oil/20% water) as a single dose at a dose volume of 10 mg/mL. Doses administered were 50, 300, and 1800 mg/kg of body weight. All toxicology animals were euthanized for postmortem examinations on study day 15, which was 14 days after dose was administered. A general physical exam was conducted on all animals prior to assignment to study. Subsequently, all animals were examined twice daily for morbidity, mortality, injury, and availability of food and water. Beginning on day 1

after administration and continuing through the day of scheduled euthanasia, examinations of general signs of toxicity, including fecal and urine quality, were conducted once daily. Beginning on day 1 of dosing, body weights were recorded daily until euthanasia. Post-mortem examinations were performed on all toxicology animals. At necropsy, the animals were examined visually for external abnormalities. The abdominal, thoracic, and cranial cavities and their contents were examined for abnormalities and the liver and kidneys removed and examined. Prenecropsy fasted body weights were examined as well as necropsy weights of the liver and paired kidneys.

Acknowledgment. We acknowledge the following individuals and organizations for their contributions to the work described in this manuscript: Wuxi AppTec; ReachBio LLC; BASi; and Dr. Patrick Carroll, University of Pennsylvania.

References

(1) *Hepatitis C*; World Health Organization Fact Sheet No. 164; World Health Organization: Geneva, October 2000.
(2) Lavanchy, D. The Global Burden of Hepatitis C. *Liver Int*. **2009**, *29* (S1), 74.
(3) Zeuzem, S.; Berg, T.; Moeller, B.; Hinrichsen, H.; Mauss, S.; Wedemeyer, H.; Sarrazin, C.; Hueppe, D.; Zehnter, E.; Manns, M. P. Expert Opinion on the Treatment of Patients with Chronic Hepatitis C. *J. Viral Hepatitus* **2009**, *16*, 75.
(4) Fried, M. W.; Shiffman, M. L.; Reddy, K. R.; Smith, C.; Marinos, G.; Goncales, F. L.; Haussinger, D.; Diango, M.; Carosi, G.; Dhumeaux, D.; Craxi, A.; Lin, A.; Hoffman, J.; Yu, J. *N. Engl. J. Med.* **2002**, *347*, 975–982.
(5) Burton, J. R.; Everson, G. T. HCV NS5B Polymerase Inhibitors. *Clin. Liver Dis*. **2009**, *13*, 453–465.
(6) Beaulieu, P. L. Recent Advances in the Development of NS5B Polymerase Inhibitors for the Treatment of Hepatitis C Virus Infection. *Expert Opin. Ther. Pat*. **2009**, *19*, 145–164.
(7) Simmonds, P. Genetic Diversity and Evolution of Hepatitis C Virus—15 Years On. *J. Gen. Virol*. **2004**, *85*, 3173–3188.
(8) Le Guillou-Guillemette, H.; Vallet, S.; Gaudy-Graffin, C.; Payan, C.; Pivet, A.; Goudeau, A.; Lunel-Fabiani, F. Genetic Diversity of the Hepatitis C Virus: Impact and Issues in the Antiviral Therapy. *World J. Gastroenterol*. **2007**, *13*, 2416–2426.
(9) Pierra, C.; Amador, A.; Benzaria, S.; Cretton-Scott, E.; D'Amours, M.; Mao, J.; Mathieu, S.; Moussa, A.; Bridges, E. G.; Standring, D. M.; Sammadossi, J.-P.; Storer, R.; Gosselin, G. Synthesis and Pharmacokinetics of Valopicitabine (NM283), an Efficient Prodrug of the Potent Anti-HCV Agent 2′-*C*-Methylcytidine. *J. Med. Chem*. **2006**, *49*, 6614–6620.
(10) Smith, D. B.; Kalayanov, G.; Sund, G.; Winqvist, A.; Maltseva, T.; Leveque, V. J.-P.; Rajyagurr, S.; Le Pogam, S.; Najer, I.; Benkestock, K.; Zhou, X.-X.; Kaiser, A. C.; Maag, H.; Cammack, N.; Martin, J. A.; Swallow, S.; Johannsson, N. G.; Klumpp, K.; Smith, M. The Design, Synthesis, and Antiviral Activity of Monofluoro and Difluoro Analogues of 4′-Axidocytidine against Hepatitis C Virus Replication: The Discovery of 4′-Azido-2′-deoxy-2′-fluorocytidine and 4′-Azido-2′-dideoxy-2′,2′-difuorocytidine. *J. Med. Chem*. **2009**, *52*, 2971–2978.
(11) Clark, J. L.; Hollecker, L.; Mason, J. C.; Stuyver, L. J.; Tharnish, P. M.; Lostia, S.; McBrayer, T. R.; Schinazi, R.; Watanabe, K. A.; Otto, M. J.; Furman, P. A.; Stec, W. J.; Patterson, S. E.; Pankiewicz, K. W. Design, Synthesis, and Antiviral Activity of 2′-Deoxy-2′-fluoro-2′-*C*-methylcytidine, a Potent Inhibitor of Hepatitis C Virus Replication. *J. Med. Chem*. **2005**, *48*, 5504–5508.
(12) Stuyver, L. J.; McBrayer, T. R.; Tharnish, P. M.; Clark, J. L.; Hollecher, L.; Lostia, S.; Nachman; Grier, J.; Bennett, M. A.; Xie, M.-Y.; Schinazi, R. F.; Morrey, J. D.; Julander, J. L.; Furman, P. A.; Otto, M. J. Inhibition of Hepatitis C Replicon RNA Synthesis by β-D-2′-Deoxy-2′-fluoro-2′-*C*-methylcytidine: A Specific Inhibitor of Hepatitis C Virus Replication. *Antiviral Chem. Chemother*. **2006**, *17*, 79–87.
(13) Stuyver, L. J.; McBrayer, T. R.; Whitaker, T.; Tharnish, P. M.; Ramesh, M.; Lostia, S.; Cartee, L.; Shi, J.; Hobbs, A.; Schinazi, R. F.; Watanabe, K. A; Otto, M. J. Inhibition of the Subgenomic Hepatitis C Virus Replicon in Huh-7 Cells by 2′-Deoxy-2′-fluoro Cytidine. *Antimicrob. Agents Chemother*. **2004**, *48*, 651–654.
(14) Reddy, R.; Rodriguez-Torres, M.; Gane, E.; Robson, R.; Lalezari, J.; Everson, G.; DeJesus, E.; McHutchinson, J.; Vargas, H. Presented at the 58th Annual Meeting of the American Association of the Study of Liver Disease, Boston, November 2007; Abstract LB9; unpublished results.
(15) Lalezari, J.; Gane, E.; Rodriguez,-Torres, M.; DeJesus, E.; Nelson, D.; Everson, G.; Jacobson, I.; Reddy, R.; Hill, G. Z.; Beard, A.; Symonds, W. T.; Berrey, M. M.; McHutchison, J. G. Potent Antiviral Activity of the HCV Nucleoside Polymerase Inhibitor R7128 with PEG-INF and Ribavirin: Interim Results of R7128 500 mg BID for 28-Days. Presented at the 43rd Annual Meeting of the European Association for the Study of the Liver, Milan, Italy, April 2008; unpublished results.
(16) Rodriguez-Torres, M.; Lalezari, J; Gane, E.; DeJesus, E.; Nelson, D.; Everson, G.; Jacobsen, I.; Reddy, R.; McHutchinson, J.; Beard, A.; Walker, S.; Symonds, B.; Berrey, M. Potent Antiviral Response to the HCV Nucleoside Polymerase Inhibitor R7128 for 28 Days with PEG-INF and Ribavirin: Subanalysis by Race/Ethnicity, Weight and HCV Genotype. Presented at the 59th Annual Meeting of the American Association for the Study of Liver Disease, San Francisco, CA, November 2008; Abstract No. 1899; unpublished results.
(17) Ma, H.; Jiang, W. R.; Roblendo, N.; Leveque, V.; Ali, S.; Lara-Jaime, T.; Masjedizdeh, M.; Smith, D. B.; Cammack, N.; Klumpp, K.; Symons, J. Characterization of the Metabolic Activation of Hepatitis C Virus Nucleoside Iinhibitor beta-D-2′-Deoxy-2′-fluoro-2′-*C*-methylcytidine (PSI-6130) and Identification of a Novel active 5′-Triphosphate Species. *J. Biol. Chem*. **2007**, *282*, 29812–29820.
(18) Murakami, E.; Bao, H.; Ramesh, M.; McGrayer, T. R.; Whitaker, T.; Micolochick Steuer, H. M.; Schinazi, R. F.; Stuyver, L. J.; Obikhod, A.; Otto, M. J.; Furman, P. A. Mechanism of Activation of beta-D-2′-Deoxy-2′-fluoro-2′-*C*-methylcytidine and Inhibition of Hepatitis C Virus NS5B RNA Polymerase. *Antimicrob. Agents Chemother*. **2007**, *51*, 503–509.
(19) Murakami, E.; Niu, C.; Bao, H.; Micolochick Steuer, H. M.; Whitaker, T.; Nachman, T.; Sofia, M. J.; Wang, P.; Otto, M. J.; Furman, P. A. The Mechanism of Action of beta-D-2′-Deoxy-2′-fluoro-2′-*C*-methylcytidine Involves a Second Metabolic Pathway Leading to beta-D-2′-Deoxy-2′-fluoro-2′-*C*-methyluridine 5′-Triphosphate, a Potent Inhibitor of the Hepatitis C Virus RNA-Dependent RNA Polymerase. *Antimicrob. Agents Chemother*. **2008**, *52*, 458–464.
(20) McGuigan, C.; Cahard, D.; Sheeka, H. M.; De Clercq, E.; Balzarini, J. Aryl Phosphoramidate Derivatives of d4T Have Improved Anti-HIV Efficacy in Tissue Culture and May Act by the Generation of a Novel Intracellular Metabolite. *J. Med. Chem*. **1996**, *39*, 1748–1753.
(21) McGuigan, C.; Sutton, P. W.; Cahard, D.; Turner, K.; O'Leary, G.; Wang, Y.; Gumbleton, M.; De Clercq, E.; Balzarini, J. Synthesis, Anti-Human Immunodeficiency Virus Activity and Esterase Lability of Some Novel Carboxylic Ester-Modified Phosphoramidate Derivatives of Stavudine (d4T). *Antiviral Chem. Chemother*. **1998**, *9*, 473–479.
(22) Saboulard, D.; Naesens, L.; Cahard, D.; Salgado, A.; Pathirana, R.; Velazquez, S.; McGuigan, C.; De Clercq, E.; Balzarini, J. Characterization of the Activation Pathway of Phosphoramidate Triester Prodrugs of Stavudine and Zidovudine. *Mol. Pharmacol*. **1999**, *56*, 693–704.
(23) Perrone, P.; Daverio, F.; Valente, R.; Rajyaguru, S.; Martin, J. A.; Lévêque, V.; Le Pogam, S.; Najera, I.; Klumpp, K.; Smith, D. B.; McGruigan, C. First Example of Phosphoramidate Approach Applied to a 4′-Substituted Purine Nucleotide (4′-Azidoadenosine): Conversion of an Inactive Nucleotide to a Submicromolar Compound versus Hepatitis C Virus. *J. Med. Chem*. **2007**, *50*, 55463–5470.
(24) McGuigan, C.; Kelleher, M. R.; Perrone, P.; Mulready, S.; Luoni, G.; Daverio., F.; Rajyaguru, S.; Le Pogam., S.; Najer, I.; Martin, J. A.; Klumpp, K.; Smith, D. B. The Application of Phosphoramidate ProTide Technology to the Potent Anti-HCV Compound 4′-Azidocytidine (R1479). *Bioorg. Med. Chem. Lett*. **2009**, *19*, 4250–4254.
(25) Gardelli, C.; Attenni, B.; Donghi, M.; Meppen, M.; Pacini, B.; Harper, S.; Di Marco, A.; Fiori, F.; Giuliano, C.; Pucci, V.; Laufer, R.; Gennari, N.; Marcucci, I.; Leone, J. F.; Olsen, D. B.; MacCoss, M.; Rowley, M.; Narjes, F. Phosphoramidate Prodrugs of 2′-*C*-Methylcytidine for the Therapy of Hepatitis C Virus Infection. *J. Med. Chem*. **2009**, *52*, 5394–5407.
(26) Wang, P.; Chin, B.-K.; Rachakonda, S.; Du, J.; Khan, N.; Shi, J.; Stec, W.; Cleary, D.; Ross, B. S.; Sofia, M. J. An Efficient and Diastereoselective Synthesis of PSI-6130: A Clinically Efficacious Inhibitor of HCV NS5B Polymerase. *J. Org. Chem*. **2009**, *74*, 6819–6824.
(27) Chen, J.; Jian, J.; Zhang, F.; Yu, H.; Zhang, J. Cytotoxic Effects of Environmentally Relevant Chlorophenols on L929 Cells and Their Mechanism. *Cell Biol. Toxicol*. **2004**, *20*, 183–196.

(28) Phornchirasilp, S.; Victor DeSouza, J. J.; Feller, D. R. Vivo and In Vitro Studies of the Hepatotoxic Effects of 4-Chlorophenol in Mice. *Biochem. Pharmacol.* **1989**, *38*, 961–972.
(29) Zhao, F.; Mayura, K.; Hutchinson, R. W.; Lewis, R. P.; Burghardt, R. C.; Phillips, T. D. Developmental Toxicity and Structure−Activity Relationships of Chlorophenols Using Human Embryonic Palatal Mesenchymal Cells. *Toxicol. Lett.* **1995**, *78*, 35–42.
(30) Niu, C.; Murakami, E.; Furman, P. A. Clevudine Is Efficiently Phosphorylated to the Active Triphosphate Form in Primary Human Hepatocytes. *Antiviral Ther.* **2008**, *13*, 263–269.
(31) Ghose, A. K.; Viswanadhan, V. N.; Wendoloski, J. J. Prediction of Hydrohobic Properties of Small Organic Molecules Using Fragment Methods: An Analysis of AlogP and ClogP Methods. *J. Phys. Chem. A* **1998**, *102*, 3762–3772.
(32) Faller, B. Artificial Membrane Assays To Assess Permeability. *Curr. Drug Metab.* **2008**, *9*, 886–892.
(33) Fleischer, R. l.; Lok, A. S. Myopathy and Neuropathy Associated with Nucleos(t)ide Analog Therapy for Hepatitis B. *J. Hepatol.* **2009**, *51*, 787–791.
(34) Lewis, W.; Day, B. J.; Copeland, W. C. Mitochondrial Toxicity of NRTI Antiviral Drugs: An Integrated Cellular Perspective. *Nat. Rev. Drug Discovery* **2003**, *2*, 812–822.
(35) Sammadossi, J. P.; Carlisle, R. Toxicity of 3′-Azido-3′-deoxythymidine and 9-(1,3-Dihydroxy-2-propoxymethyl)guanine for Normal Human Hematopoietic Cells in Vitro. *Antimicrob. Agents Chemother.* **1987**, *31*, 452–454.
(36) Sammadossi, J. P.; Schinazi, R. F.; Chu, C. K.; Xie, M. Y. Comparison of Cytotoxicity of the (−)- and (+)-Enantiomer of 2′,3′-Dideoxy-3′-thiacytidine in Normal Human Bone Marrow Progenitor Cells. *Biochem. Pharmacol.* **1992**, *44*, 1921–1925.
(37) (a) Sofia, M. J.; Du, J.; Wang, P.; Nagarathnam, D. Nucleoside Phosphoramidate Prodrugs. WO2008121634, 2008.
(38) Migliaccio, G.; Tomassini, J. E.; Carroll, S. S.; Tomei, L.; Altamura, S.; Bhat, B.; Bartholomew, L.; Gosserman, M. R.; Ceccacci, A.; Colwell, L. F.; Cortese, R.; Eldrup, A. B.; Getty, K. L.; Hou, X. S.; LaFemina, R. L.; Ludmerer, S. W.; MacCoss, M.; McMasters, D. R.; Stahlhut, M. W.; Olsen, D. B.; Hazuda, D. J.; Flores, O. A. Characterization of Resistance to Non-Obligate Chain-Terminating Ribonucleoside Analogs That Inhibit Hepatitis C Virus Replication in Vitro. *J. Biol. Chem.* **2003**, *278*, 49164–49170.
(39) Le Pagam, S.; Jiang, W.-R.; Leveque, V.; Rajyaguru, S.; Ma, H.; Kang, H.; Jiang, S.; Singer, M.; Ali, S.; Klumpp, K.; Smith, D.; Symons, J.; Cammack, N.; Najera, I. In Vitro Selected Con1 Subgenomic Replicons Resistant to 2′-*C*-Methyl-cytidine or to R1479 Show Lack of Cross Resistance. *Virology* **2006**, *351*, 349–359.
(40) Ali, S.; Leveque, V.; Le Pogam, S.; Ma.; Philipp, F.; Inocencio, N.; Smith, M.; Alker, A.; Kang, H.; Najera, I.; Klumpp, K.; Symons, J.; Cammack, N.; Jiang, W. R. Selected Replicon Variants with Low-Level in Vitro Resistance to the Hepatitis C Virus NS5B Polymerase Inhibitor PSI-6130 Lack Cross-Resistance with R1479. *Antimicrob. Agents Chemother.* **2008**, *52*, 4356–4369.
(41) Altomare, A.; Burla, M.; Camalli, G.; Cascarano, G.; Giacovazzo, C.; Guagliardi, A.; Moliterni, A.; Polidori, G.; Spagna, R. SIR97: A New Tool for Crystal Structure Determination and Refinement. *J. Appl. Crystallogr.* **1999**, *32*, 115–116.
(42) Sheldrick, G. M. A Short History of SHELX. *Acta Crystallogr.* **2008**, *A64*, 112–122.
(43) Stuyver, L. J.; Lostia, S.; Adams, M.; Mathew, J. S.; Pai, B. S.; Grier, J.; Tharnish, P. M.; Choi, Y.; Chong, Y.; Choo, H.; Chu, C. K.; Otto, M. J.; Schinazi, R. F. Antiviral Activities and Cellular Toxicities of Modified 2′,3′-Dideoxy-2′,3′-didehydrocytidine Analogues. *Antimicrob Agents Chemother.* **2002**, *46*, 3854–3860.